Extrinsic cues cooperate with intrinsic temporal factors to increase neuronal diversity

Anthony M. Rossi and Claude Desplan*

Department of Biology, New York University, New York, NY 10003, USA.

*lead contact

Correspondence: amr808@nyu.edu, cd38@nyu.edu

Summary:

How diverse neuronal types are sequentially generated from individual neural stem cells is a central question in neurobiology. This "temporal patterning" is controlled by both intrinsic and extrinsic cues. Whether and how extrinsic cues interact with intrinsic programs to increase neuronal diversity, or if they only fine-tune the timing of temporal transitions, is not known. We use the simple *Drosophila* mushroom body lineage, comprised of only three neuronal types that are sequentially produced, to address the role of extrinsic cues in temporal patterning. As they age, mushroom body stem cells (neuroblasts) advance through intrinsic and opposing temporal gradients of two RNA-binding proteins, Imp and Syp. These intrinsic gradients are used to first produce γ, then α'β', and finally αβ neurons. The specification of each neuronal type is temporally confined to specific developing stages, and progression from one temporal window to the next occurs concurrently with key, developmental events. This suggests that extrinsic cues play important roles in patterning temporal identity in this lineage. We show that an extrinsic cue, Activin, not only times the young (Imp) to old (Syp) neuroblast fate transition but that it is also essential for increasing neuronal diversity by defining the mid-temporal window (α'β'). Activin reduces the levels of the intrinsic factor Imp, creating a scenario where Imp and Syp are both at low levels for an extended period. In Activin receptor mutants, α'β' neurons are not generated because high Imp levels inhibit the activation of α'β' effectors, including ecdysone receptor signaling. Additionally, the γ temporal window appears to be extended and the αβ window is shortened, due to a delayed Imp to Syp transition. Our results illustrate that temporal extrinsic cues during neurogenesis can modify an intrinsic temporal program to increase neuronal diversity.

Keywords:

Temporal patterning, neuronal specification, intrinsic, extrinsic, *Drosophila*, mushroom body, Kenyon cells, RNA-binding, Activin, ecdysone

Introduction:

The building of intricate neural networks during development is controlled by highly coordinated patterning programs that regulate the generation of different neuronal types in the correct number, place and time. The sequential production of different neuronal types is a conserved feature of neurogenesis and is called temporal patterning (Holguera and Desplan, 2018; Kohwi and Doe, 2013). We study temporal patterning in *Drosophila* neural stem cells, called neuroblasts, and focus on how intrinsic and extrinsic temporal mechanisms converge to control the generation of neuronal diversity.

The first insights into intrinsic mechanisms of temporal patterning were discovered in *Drosophila* embryonic ventral nerve cord (VNC) neuroblasts, which produce neurons that are the functional equivalent to those in the vertebrate spinal cord (Brody and Odenwald, 2000; Doe, 2017; Grosskortenhaus et al., 2005, 2006; Isshiki et al., 2001; Kambadur et al., 1998; Kohwi and Doe, 2013; Pearson and Doe, 2003; Tran and Doe, 2008). VNC neuroblasts produce a large number of unique neuronal types. To achieve this, each neuroblast sequentially expresses a series of temporal transcription factors (tTFs) as it ages, with each tTF being expressed for only 1-2 cell divisions. Neurons born within each tTF window are endowed with a specific temporal identity. Postembryonic neuroblasts in the *Drosophila* optic lobes and intermediate neural progenitors (INPs) born from specialized neuroblasts in the central brain (called Type II neuroblasts) also produce highly diverse sets of neurons sequentially (Abdusselamoglu et al., 2019; Bayraktar and Doe, 2013; Bello et al., 2008; Bertet et al., 2014; Boone and Doe, 2008; Bowman et al., 2008; Eroglu et al., 2014; Li et al., 2013; Suzuki et al., 2013). Once again, they rapidly progress through a tTF series, although the identity of the tTFs differ from those in the VNC. In all of these examples, advancement through a tTF series is quick and intrinsic, such that interactions among tTFs allow neuroblasts to progress through successive temporal windows without the need for extrinsic input (Averbukh et al., 2018; Doe, 2017; Rossi et al., 2017).

The majority of postembryonic central brain neuroblasts produce a large number of neuronal types like the neuroblasts in the embryonic VNC or optic lobes but do so over the course of many days, many more cell divisions, and multiple developmental stages, leading to larger lineages (Miyares and Lee, 2019; Wang et al., 2014; Yu et al., 2010, 2013). Rapidly progressing tTF series have not been described in central brain neuroblasts. Although such tTFs are likely to exist in these neuroblasts, they also use a different type of temporal patterning mechanism, one that incorporates both intrinsic and extrinsic cues. They express two RNA-binding proteins in highly extended and opposing temporal gradients, *IGF-II mRNA binding protein* (*Imp*) when they are young and *Syncrip* (*Syp*) when they are old (Dillard et al., 2018; Genovese et al., 2019; Liu et al., 2015; Ren et al., 2017; Syed et al., 2017a), defining two broad temporal windows. Inhibition between Imp and Syp contributes, but is not sufficient, to account for the transition from young (Imp) to old (Syp) states (Dillard et al., 2018; Liu et al., 2015; Ren et al., 2017; Syed et al., 2017b, 2017a). A factor that is necessary for this absolute transition is Seven-Up (Svp), which is part of an intrinsic temporal series and is transiently expressed early during the Imp temporal window (Ren et al., 2017; Syed et al., 2017a). In the absence of Svp, neuroblasts remain forever young and continuously express Imp. Extrinsic input acts within this intrinsic program, as Svp is necessary for the expression of the Ecdysone receptor (EcR), a nuclear hormone receptor, in neuroblasts (Syed et al., 2017a). Ecdysone is responsible for major developmental transitions, including the transitions between the three larval stages, entry into pupation, and for eclosion (Yamanaka et al., 2013). Ecdysone fine-tunes the timing of the Imp to Syp switch but, unlike Svp, it is not necessary for it as inhibiting ecdysone reception only leads to a delay in the transition, which causes an increase of the number of cells with a young identity (Dillard et al., 2018; Syed et al., 2017a).

One question that has remained unanswered is whether extrinsic cues play a role beyond timing temporal identity transitions in neuroblasts and if they can also contribute to the generation of neuronal diversity (Kawaguchi, 2019; Syed et al., 2017b). To address this question, we focused on the *Drosophila* mushroom body lineage. Mushroom body neurons (Kenyon cells) are extensively studied for their roles in learning and memory (Cognigni et al., 2018). They are born from four identical neuroblasts per hemisphere, which divide continuously from the late embryonic stages until the end of pupation (~9 days for ~250 divisions each) (Figure 1A) (Ito et al., 1997; Kraft et al., 2016; Kurusu et al., 2009; Lee et al., 1999; Pahl et al., 2019; Siegrist et al., 2010; Sipe and Siegrist, 2017). Within this very long period, only three main neuronal types are produced

sequentially, first γ, followed by α'β', and then αβ (Figure 1A), representing the simplest lineage in the central brain. Because of this neuronal simplicity, the broad temporal windows defined by Imp and Syp are sufficient to define the three major neuronal types (Liu et al., 2015) and do not require further subdivision by sequences of tTFs, as in other neuroblasts. Moreover, extrinsic cues likely play an important role in patterning the three neuronal types since the timing of their specification is limited to time points between developmental stages of the animal (Figure 1A): The γ temporal window extends from L1 (the first larval stage) until mid L3 (the final larval stage) when animals attain critical weight and are committed to metamorphosis, the α'β' window from mid L3 to the beginning of pupation, and the αβ window from pupation until eclosion (the end of development) (Lee et al., 1999). Additionally, temporal window duration is affected by the nutritional status of the animal (Lin et al., 2013). For example, the γ temporal window (and the time spent in an early larval stage) is extended upon early starvation, resulting in the generation of additional γ neurons without affecting later temporal windows (Lin et al., 2013).

How broad Imp and Syp gradients pattern temporal identity is best understood in the mushroom body lineage: Imp positively and Syp negatively regulate the translation of *chronologically inappropriate morphogenesis* (*chinmo*), a transcription factor that also acts as a temporal morphogen but in mushroom body neurons, rather than in neuroblasts (Kao et al., 2012; Ren et al., 2017; Zhu et al., 2006). The first-born γ neurons are produced for the first ~85 cell divisions, when Imp levels in neuroblasts, and thus Chinmo in neurons, are high. α'β' neurons are produced for the next ~40 divisions, when Imp and Syp are at roughly equal and low levels. These lower levels of Imp in neuroblasts are important for lower Chinmo levels in neurons born at this time, which activates the expression of EcR and *maternal gene required for meiosis* (*mamo*), which itself is stabilized by Syp and required for α'β' specification (Liu et al., 2019; Marchetti and Tavosanis, 2017). αβ neurons are generated for the final ~125 neuroblast divisions, when Syp levels are high and Imp is no longer expressed. This neuronal simplicity and extensive knowledge about the intrinsic temporal patterning mechanism, coupled with tools to label and target neuronal types during development and in the adult, provided us with a unique opportunity to investigate whether and how extrinsic cues interact with an intrinsic temporal patterning mechanism to affect neuronal diversity.

Here we show that an extrinsic signal, Activin, not only times the young (Imp) to old (Syp) temporal transition but also lowers Imp levels to define the mid, α'β' temporal identity window. Inhibiting Activin signaling in mushroom body neuroblasts leads to the loss of the second-born α'β' neurons, to fewer last-born αβ neurons, and to the likely generation of additional first-born γ neurons. We uncovered the mechanism for how α'β' neurons are lost in Activin signaling mutants by showing that low Imp levels in neurons are essential for their expression of EcR, which responds to a second extrinsic cue and is necessary but not sufficient for α'β' specification, partly by controlling the activation of Mamo. Thus, we show that the sequential generation of neuronal diversity during development is controlled by the intrinsic progression of temporal factors that are modified by an extrinsic cue. These findings could help us better understand the functions of extrinsic signaling during vertebrate neurogenesis, which also incorporate extrinsic cues to control the sequential birth of neuronal types (Desai and McConnell, 2000; Dias et al., 2014; Frantz and McConnell, 1996; Kawaguchi, 2019; McConnell, 1988; Oberst et al., 2019).

Results:

α'β' neurons are not generated in *babo* and *EcR* mutants

As described above, mushroom body temporal windows are limited within developmental stages of the animal, as the γ window extends from L1 to mid L3, the α'β' window from mid L3 to pupation, and the αβ window from pupation to eclosion (Figure 1A) (Lee et al., 1999). This means that extrinsic cues could play a role in controlling or fine-tuning temporal transitions. Additionally, the specification of neuronal identity within each temporal window could be aided by extrinsic cues that change during development. To test these hypotheses, we performed a directed screen using Mosaic Analysis with Repressible Cell Marker (MARCM) (Lee and Luo, 1999), targeting inter-cellular signaling pathways with known roles either in mushroom body neurogenesis (Activin and ecdysone) (Lee et al., 2000; Zheng et al., 2003) or more broadly during nervous system development (Hedgehog and juvenile hormone) (Figure S1) (Baumann et al., 2017; Chai et al., 2013). We induced mutant neuroblast clones at L1 and compared the axonal morphologies of adult neurons born from a mutant mushroom body neuroblast to neurons born from the other wildtype mushroom body neuroblasts in the same hemisphere. To identify axonal lobes (both mutant and wildtype), we used antibodies to Trio (γ and α'β' marker) or to FasII (an axonal γ and αβ marker)

(Figure 1A') (Awasaki et al., 2000; Crittenden et al., 1998). To visualize mushroom body neurons within clones we used *OK107-Gal4* (referred to as *mb-Gal4* hereafter), a *Gal4* enhancer trap in *eyeless* and a common mushroom body *Gal4* driver that strongly labels all mushroom body neuronal types and weakly mushroom body neuroblasts throughout development (Connolly et al., 1996; Liu et al., 2015; Zhu et al., 2006). We identified the Activin type-I receptor, Baboon (Babo), and EcR, as important for the specification of the second-born α'β' neurons (Figures 1B-H, S1A-C). EcR was already known to regulate α'β' identity (Marchetti and Tavosanis, 2017).

In wildtype clones induced at L1, GFP-labeled axons projected to all five mushroom body lobes: α, α′, β, β' (hidden behind the γ lobe in max projections), and γ (Figures 1B, S1A). In *babo* and *EcR-DN* clones however, we were unable to detect GFP+ axons within the α'β' lobes, which remained visible by Trio staining due to the presence of wildtype mushroom body neurons (Figures 1C-D, S1B-C). In addition, and as previously described, mutant γ neurons remained unpruned in both mutant conditions (visualized by vertical GFP+ axons that were Trio+ and FasII+), providing a positive control for the efficiency of the mutants, since γ remodeling is known to require Babo and EcR (Figures 1C-D, S1B-C) (Lee et al., 2000; Zheng et al., 2003). Interestingly, we found that the EcR co-receptor, Ultraspiracle (Usp), was not necessary for the specification of α'β' neurons, although it was required for γ neuron remodeling, consistent with previously published reports (Figure S1D) (Lee et al., 2000). The phenotypic difference between *EcR-DN* and *usp* mutants may be due to differences in activation and/or repression of ecdysone target genes elicited by these factors, which have been shown by others (Ghbeish et al., 2001; Schubiger and Truman, 2000). To test whether α'β' neuron specification required the canonical Activin signaling pathway (Brummel et al., 1999), we induced *Smad2* mutant clones at L1 and characterized adult axonal morphologies. Smad2 is the transcriptional effector of the Activin pathway. Similar to *babo* mutant clones, *Smad2* mutant clones were missing most α'β' neurons and contained unpruned γ neurons (Figure S1J).

To test whether the absence of GFP+ axons within the α'β' lobes in *babo* and *EcR-DN* mutants was due to the loss of axonal projections or the loss of neuronal identity, we used two

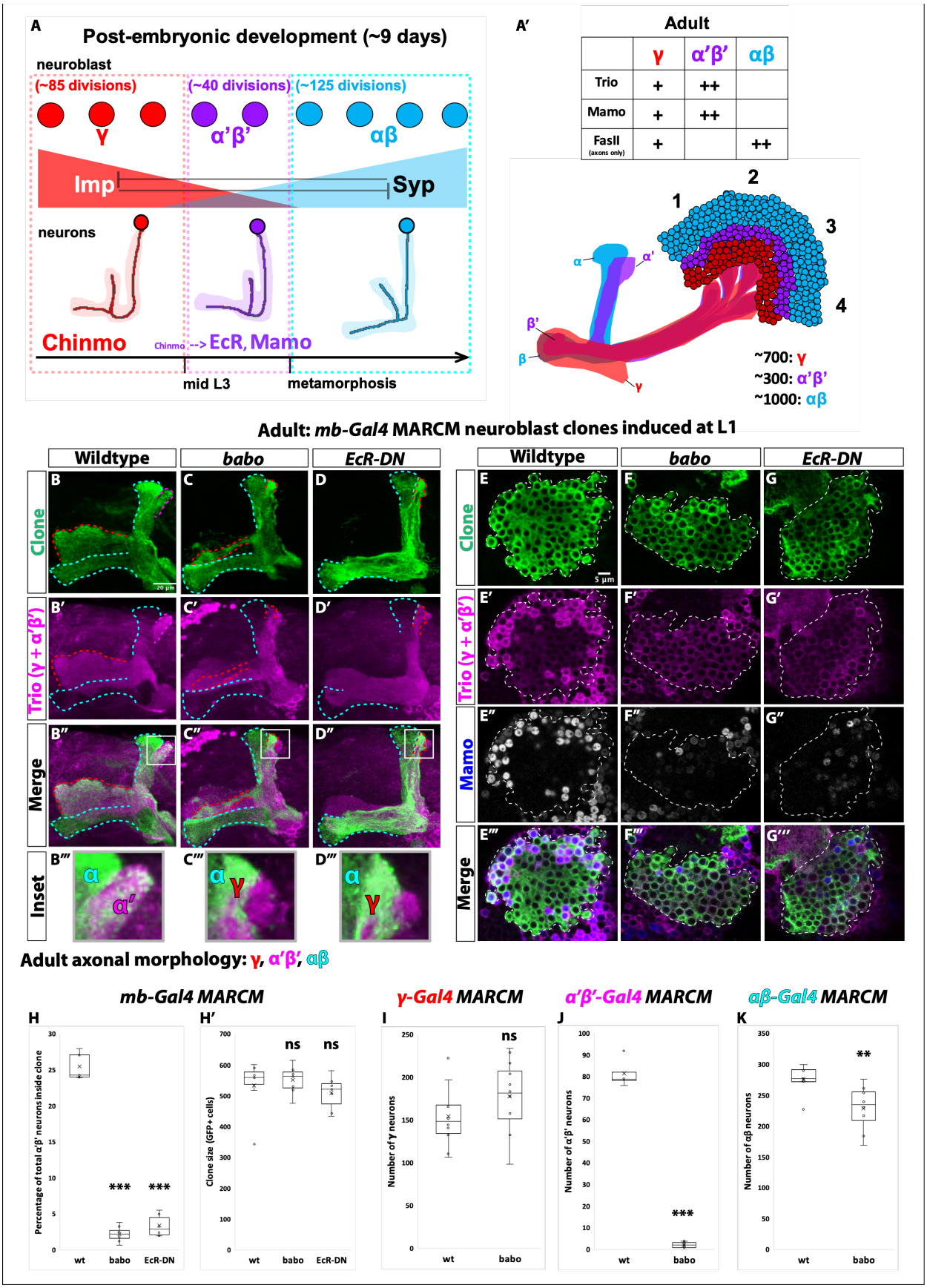
A
Post-embryonic development (~9 days)
neuroblast
(~85 divisions)
(~40 divisions)
(~125 divisions)
γ
α'β'
αβ
Imp
Syp
neurons
Chinmo
Chinmo --> EcR, Mamo
mid L3
metamorphosis
A'
Adult
γ
α'β'
αβ
Trio
+
++
Mamo
+
++
FasII (axons only)
+
++
1
2
3
4
α
α'
β'
β
γ
~700: γ
~300: α'β'
~1000: αβ
Adult: mb-Gal4 MARCM neuroblast clones induced at L1
Wildtype
babo
EcR-DN
Clone
Trio (γ + α'β')
Merge
Inset
B
C
D
B'
C'
D'
B''
C''
D''
B'''
C'''
D'''
α
α'
γ
20 µm
E
F
G
E'
F'
G'
E''
F''
G''
E'''
F'''
G'''
Mamo
5 µm
Adult axonal morphology: γ, α'β', αβ
mb-Gal4 MARCM
γ-Gal4 MARCM
α'β'-Gal4 MARCM
αβ-Gal4 MARCM
H
H'
I
J
K
Percentage of total α'β' neurons inside clone
Clone size (GFP+ cells)
Number of γ neurons
Number of α'β' neurons
Number of αβ neurons
wt
babo
EcR-DN
***
ns
**

Figure 1. Activin and ecdysone signaling are necessary for the specification of α'β' neurons. A. Summary of mushroom body development. During early larval stages, mushroom body neuroblasts express high levels of Imp (red) and Chinmo (red) to specify γ neurons for ~85 neuroblast divisions (red-dashed box). From mid L3 to metamorphosis, when Imp and Syp (cyan) are both at low levels, the same neuroblast divides ~40 times to produce α'β' neurons (magenta-dashed box). Low Chinmo levels regulate the expression of EcR and Mamo, determinants of α'β' identity. From the beginning of metamorphosis throughout pupal development, high Syp without Imp leads to αβ neurons (cyan-dashed outline). **A'.** Known molecular markers can distinguish between the three mushroom body neuronal types in the adult. Mushroom body projections originating from neurons born from four neuroblasts (numbered 1 to 4) per hemisphere fasciculate into a single bundle (peduncle) before branching into the five mushroom body lobes. The first-born γ neurons (red) remodel during development to project into a single, medial lobe in the adult. This lobe is the most anterior of the medial lobes. Axons from α'β' neurons (magenta) bifurcate to project into the vertical and medial α' and β' lobes. The β' lobe is posterior to the γ lobe. The last-born αβ neurons (cyan) also bifurcate their axons into the vertical projecting α lobe and medial projecting β lobe. The α lobe is positioned adjacent and medial to the α' lobe. The β lobe is the most posterior medial lobe. **B-D.** Representative max projections showing adult axonal projections of clonally related neurons born from L1 stage in wildtype, *babo*, and *EcR-DN* conditions. *UAS-CD8::GFP* is driven by *mb-Gal4* (*OK107-Gal4*). Outlines mark GFP+ axons, where γ axons are outlined in red, α'β' axons are outlined in magenta, and αβ axons are outlined in cyan. A white box outlines the Inset panel. Trio (magenta) is used to label all γ and α'β' axons for comparison to GFP+ axons. **B.** In wildtype, GFP+ axons (green, outlined in red, magenta and cyan) are visible in all observable mushroom body lobes. **C.** In *babo* mutants, γ neurons (red outline) remain unpruned. GFP+ axons are missing inside the Trio+ α' lobe, indicating the absence of α'β' neurons. **D.** The same loss of α'β' axons, and the defect in γ neuron remodeling, are observed in *EcR-DN* expressing clones. **E-G.** Representative, single z-slice from the adult cell body region of clones induced at L1 in wildtype, *babo* and *EcR-DN* conditions. *UAS-CD8::GFP* is driven by *mb-Gal4*. **E.** Wildtype clones show the presence of strongly expressing Trio (magenta) and Mamo (blue, gray in single channel) neurons, indicative of α'β' identity. **F.** In *babo* mutant clones, cells strongly expressing Trio and Mamo are not present. **G.** Similarly, in *EcR-DN* clones, strong Trio and Mamo cells are not present. **H.** Quantification of MARCM clones marked by *mb-Gal4*, which labels all mushroom body neuronal types. The number of α'β' neurons are quantified in wildtype (n=7), *babo* (n=8) and *EcR-DN* (n=6) conditions. Plotted is the percentage of strong Mamo and GFP+ cells (clonal cells) versus all Mamo+ cells (clonal and non-clonal cells) within a single mushroom body. In wildtype, 25.5% of the total strong Mamo expressing cells (α'β' neurons) are within a clone, consistent with our expectation since each mushroom body is made from four neuroblasts. In *babo* clones, only 2.2% of α'β' neurons are within a clone. In *EcR-DN* clones, only 3.4% of α'β' neurons are within a clone. **H'.** There are no significant differences between the average clone sizes (wildtype:533.6, *babo*:551.3, *EcR-DN*:509.1) in the three conditions. **I.** Quantification of γ neurons marked by *γ-Gal4* (*71G10-Gal4*) in MARCM clones. Plotted is the total number of γ neurons marked by GFP and Trio in wildtype (n=10) and *babo* mutant (n=12) clones. In wildtype, the average number of γ neurons is 154.3. In *babo* mutants, the average is 178.4. **J.** Quantification of α'β' neurons marked by *α'β'-Gal4* (*41C07-Gal4*) in MARCM clones. Plotted is the total number of α'β' neurons marked by GFP and strong Trio in wildtype (n=4) and *babo* mutant (n=8) clones. In wildtype, the average number of α'β' neurons is 81.5. In *babo* mutants, the average is 2.1. **K.** Quantification of αβ neurons marked by *αβ-Gal4* (*44E04-Gal4*) in MARCM clones. Plotted is the total number of GFP+ cells in wildtype (n=7) and *babo* mutant (n=8) clones. In wildtype, the average number is 276. In *babo* mutants, the average number is 228.9. In all cases, whisker plots represent the minimum value (bottom whisker), first quartile (bottom of box to middle line), inclusive median (middle line), third quartile (middle line to top of box) and maximum value (top whisker). The "x" represents the average value. Outliers are 1.5 times the distance from the first and third quartile. For **H** and **H'**, a Tukey test was performed. Reported significance is compared to wildtype. For **I**-**K** a two-sample, two-tailed t-test was performed. ***p<0.001, **p<0.01, ns: not significant.

antibodies against molecular markers that strongly label α'β' neuron cell bodies in the adult: Trio and Mamo (Figures 1A', S1N) (Alyagor et al., 2018; Awasaki et al., 2000; Croset et al., 2018; Liu et al., 2019). In wildtype clones induced at L1 and analyzed in the adult, we detected strong Trio+ and Mamo+ cells within GFP+ clones (Figures 1E, S1K). In both *babo* and *EcR-DN* mutant clones however, the vast majority of strong Trio+ and Mamo+ cells inside clones were missing compared to surrounding wildtype mushroom body neurons (Figures 1F-G, S1L-M). We quantified this phenotype in wildtype, *babo* and *EcR-DN* clones by counting the number of Mamo+ cells within a clone versus the total number of Mamo+ cells outside the clone but within the same hemisphere.

In wildtype MARCM clones affecting a single mushroom body neuroblast (n=7), the percentage of α'β' neurons within clones was 25.5%, the expected ratio since each mushroom body is built from four identical neuroblasts (Figure 1H) (Ito et al., 1997; Lee et al., 1999). In comparison, in *babo* (n=8) and *EcR-DN* (n=6) clones, the percentage of α'β' neurons within clones was 2.2% and 3.4%, respectively (Figure 1H). These data show that both Babo and EcR are necessary for α'β' specification.

We next sought to determine the fate of the missing α'β' neurons in *babo* and *EcR-DN* clones, particularly since there was no significant difference in average clone size between wildtype and mutant clones (wildtype: n=7, clone size= 533.6; *babo*: n=7, clone size = 551.3; *EcR-DN*: n=7, clone size = 509.1) (Figure 1H'). First, we tested whether cell death played a role in the loss of α'β' neurons by expressing the caspase inhibitor P35 in *babo* and *EcR-DN* clones (Figures S2A-B). In both cases, there were still no α'β' neurons based on axonal morphology (Figures S2A-B), indicating that α'β' neurons are not generated in these mutant conditions, and that they are not born and then die. Next, we tested whether either the γ or αβ temporal window became extended in these mutant conditions. It has recently been shown that expression of EcR-DN in the mushroom body during development leads to an increased number of last-born αβ neurons (Marchetti and Tavosanis, 2017). To determine whether a similar outcome occurs in a *babo* mutant, we made MARCM clones in which either γ, α'β' neurons or αβ neurons were specifically marked, and then quantified the total number of GFP+ neurons in wildtype versus *babo* mutant conditions (Figures 1I-K, S2C-N). Using a γ driver, *R71G10-Gal4* (referred to as *γ-Gal4*), the average number of γ neurons marked by GFP and Trio increased in *babo* mutants, although not significantly (wildtype: n=10, 154.3; *babo*: n=12, 178.4) (Figures 1I, S2C-F) (Issman-Zecharya and Schuldiner, 2014). α'β' neurons, marked by *41C07-Gal4* (referred to as *α'β'-Gal4*) and by strong Trio, were almost entirely missing in *babo* mutants compared to wildtype clones (wildtype: n=4, 81.5; *babo*: n=8, 2.1) consistent with our previous results in *babo* clones marked by *mb-Gal4* (Figures 1J, 1H, S2G-J). The average number of αβ neurons, marked by *44E04-Gal4* (referred to as *αβ-Gal4*), was significantly reduced in *babo* versus wildtype clones (wildtype: n=7, 276; *babo*: n=8, 228.9) (Figures 1K, S2K-N). Together, these results suggest that additional γ neurons are produced, and show that fewer αβ neurons are generated, in a *babo* mutant. It is likely that the increase in the number of γ neurons was not significant because this population is very sensitive to the timing of

our clone induction (and thus variation between clones is large), unlike the number of α'β' and αβ neurons (see Methods).

Babo, but not EcR, acts in neuroblasts to affect the Imp to Syp ratio by lowering Imp

It has been proposed that α'β' neuronal specification depends on the inheritance of roughly equal amounts of the two RNA binding proteins, Imp and Syp, from mushroom body neuroblasts (Liu et al., 2015). Given that α'β' neurons were missing in *babo* and *EcR-DN* mutants, we asked whether these extrinsic signaling pathways act through or in parallel to Imp and Syp levels. To test this, we induced MARCM clones for *babo* or *EcR-DN* at L1 and compared the Imp to Syp ratio in

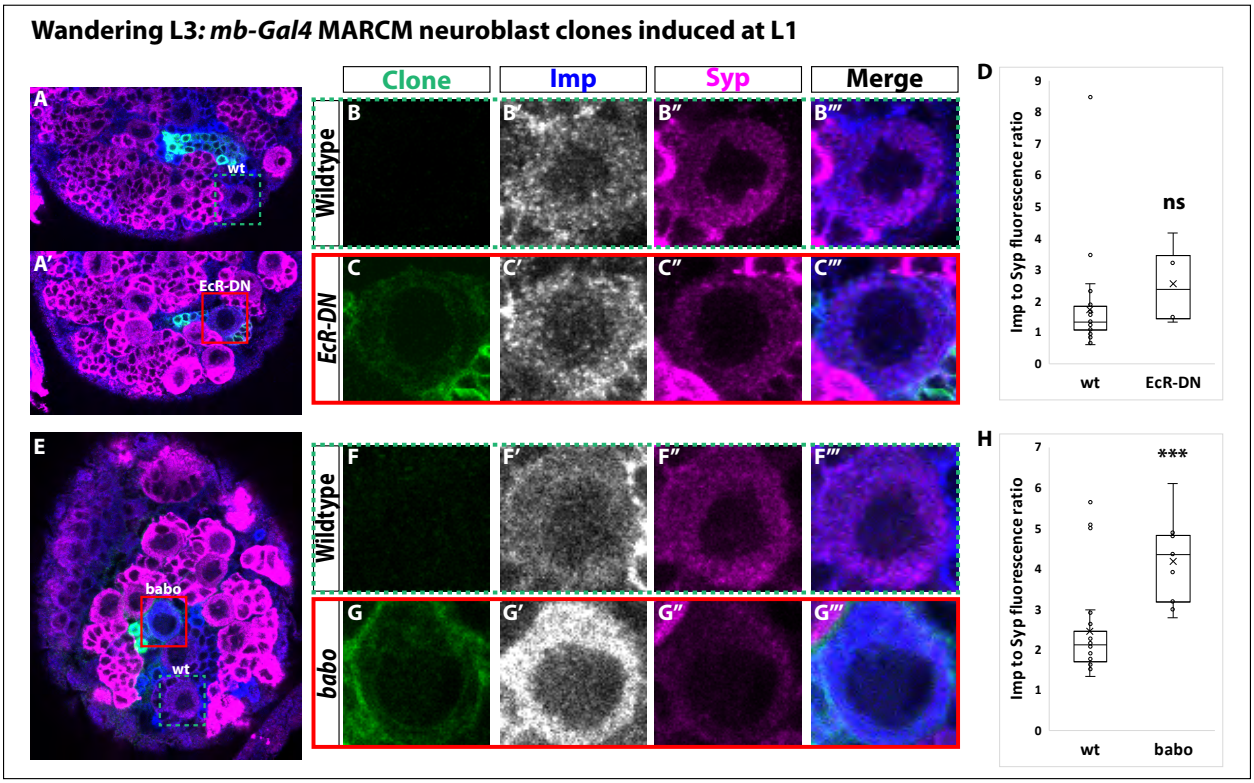

Figure 2. Extrinsic signaling through Babo, but not EcR, affects the Imp to Syp ratio in mushroom body neuroblasts. A-A'. Representative image of an *EcR-DN* neuroblast marked by *UAS-CD8::GFP* driven by *mb-Gal4* (red box) ventral to a wildtype neuroblast (green-dashed box) from the same wandering L3 stage brain, immunostained for Imp (blue, gray in single channel) and Syp (magenta). **B.** Close-up view of wildtype neuroblast (green-dashed box in **A**). **C.** Close-up view of *EcR-DN* neuroblast (red box in **A'**). **D.** Quantification of the Imp to Syp ratio in *EcR-DN* neuroblasts (n=4 from 4 different brains) compared to wildtype (n=27 from the same 4 brains as *EcR-DN* neuroblasts). **E.** Representative image of a *babo* mushroom body neuroblast marked by *UAS-CD8::GFP* driven by *mb-Gal4* (red box) adjacent to a wildtype neuroblast (green-dashed box) in the same focal plane from a wandering L3 stage brain, immunostained for Imp (blue, gray in single channel) and Syp (magenta). **F.** Close-up view of wildtype neuroblast (green-dashed box in **E**). **G.** Close up view of *babo* mutant neuroblast (red box in **E**). **H.** Quantification of Imp to Syp ratio in *babo* neuroblasts (n=9 from 4 different brains) compared to wildtype (n=23 from the same 4 brains as *babo* neuroblasts). Data in **D** and **H** are plotted as whisker plots with the same constraints as in Figure 1. A two-sample, two-tailed t-test was performed. ***$p<0.001$, ns: not significant.

mutant mushroom body neuroblasts to surrounding wildtype neuroblasts at wandering L3, the time at which α'β' neurons are produced (Figure 2). Surprisingly, and in contrast to what has been reported for other central brain neuroblasts (Syed et al., 2017a), we did not observe a significant difference in the average Imp to Syp ratio in *EcR-DN* expressing neuroblasts (n=4 from 4 different brains, ratio: 2.6) compared to surrounding wildtype neuroblasts (n=27 from the same 4 brains as *EcR-DN*, ratio: 1.7), suggesting that EcR does not act through Imp and Syp in mushroom body neuroblasts at L3 (Figures 2A-D, S3A-A'). The average Imp to Syp ratio was however significantly higher in *babo* neuroblasts (n=9 from 4 different brains, ratio: 4.2) compared to wildtype (n=23 from the same 4 brains as *babo*, ratio: 2.4), driven by a significantly higher Imp level in mutant neuroblasts (Figures 2E-H, S3B). Syp fluorescence was not significantly lower in *babo* mutants (Figure S3B'). A significantly higher Imp to Syp ratio in *babo* mutant neuroblasts persisted even ~24 hours After Pupal Formation (APF) (wildtype: n=27 from 6 different brains, ratio=0.27; *babo*: n=7 from the same 6 brains as wildtype, ratio=0.58), once again driven by a significantly higher Imp level (Figures S3C-H). Together, these results indicate that Babo inhibits Imp (either directly or indirectly) at late larval and early pupal stages. Importantly, although Imp was higher in *babo* mutant neuroblasts and persisted longer, the absolute level of Imp still decreased significantly, while the absolute level of Syp significantly increased, when comparing mutant neuroblasts at ~24 hours APF to wandering L3 (Figures S3I-J). This demonstrates that Imp still declines and Syp still increases through time independent of Activin signaling, and that these changes are either intrinsically regulated or affected by additional extrinsic factors. These findings that Imp is higher are also consistent with our suggestion that, in *babo* mutants, additional γ neurons are produced and our result that the number of αβ neurons decreased, since Imp levels remain higher for a longer period of time and likely produce γ neurons during the α'β' time window and also at the beginning of the αβ window. The lack of α'β' neurons in a *babo* mutant, even though at ~24 hours APF Imp levels were low, indicates that α'β' neurons can only be specified from L3 to the start of pupation, a relatively narrow temporal window, perhaps because of the ecdysone peak at this time point.

EcR, but not Babo, acts in neurons to specify α'β' identity.

Our result that the Imp to Syp ratio was unaffected in *EcR-DN* expressing neuroblasts (Figures 2A-D) made us consider that EcR may not be expressed in mushroom body neuroblasts at this stage. Therefore, we characterized EcR expression in the mushroom body at L3 stage using an EcR antibody and an EcR-GFP protein trap built from a MiMIC insertion (Figures 3A-B, S4A-B). At wandering L3 stage, we could not detect EcR by EcR-GFP or EcR antibody in mushroom body

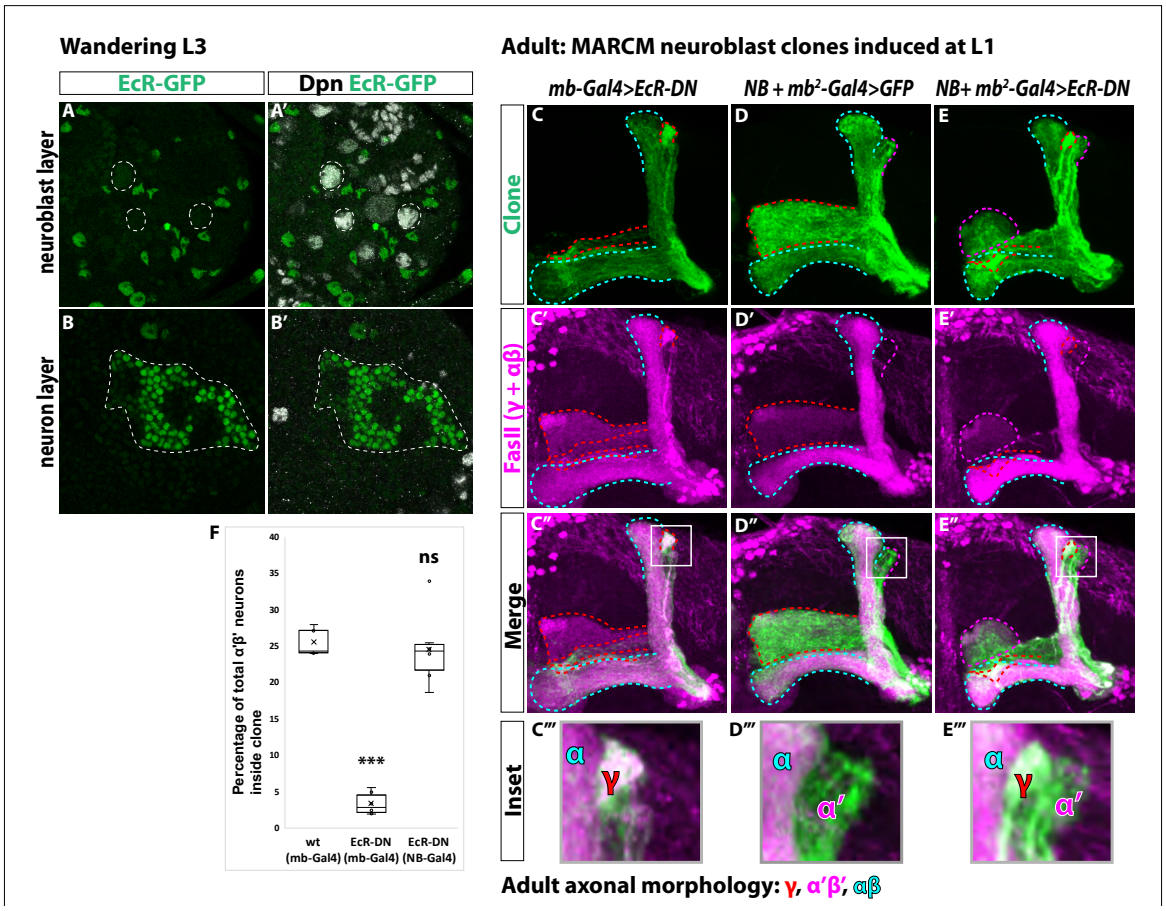

Figure 3. EcR acts in neurons to specify α'β' fate. A-A'. Mushroom body neuroblasts (white-dashed circles) marked by Dpn (gray) do not express EcR-GFP (green) at wandering L3 stage. **B-B'.** Mushroom body neurons (white-dashed outline, Dpn-) positioned ventral to the mushroom body neuroblasts in **A** express EcR-GFP. **C-E.** Outlines mark GFP+ axons, where γ axons are outlined in red, α'β' axons are outlined in magenta, and αβ axons are outlined in cyan. FasII (magenta) labels all γ and αβ axons. A gray box outlines the Inset panel. **C.** A representative adult mushroom body clone (green) induced at L1 expressing *EcR-DN* driven by *mb-Gal4*. α'β' neurons (GFP+, FasII-) are not observed and γ neurons do not remodel (GFP+, FasII+, red outline)q. **D.** A representative adult wildtype clone induced at L1 driven by *NB + mb2-Gal4*. All three neuron types are present, including α'β' neurons (GFP+, FasII-, magenta outline). **E.** α'β' neurons are also present when *EcR-DN* is driven by *NB + mb2-Gal4*. γ neurons do not remodel. **F.** Quantification of MARCM clones in which *EcR-DN* is driven by *mb-Gal4* (n=6, replotted from data in Figure 1H).) or *NB + mb2-Gal4* (n=6) compared to wildtype (n=7, replotted from data in Figure 1H). Plotted is the percentage of strong Mamo+ and GFP+ cells (clonal cells) versus all Mamo+ cells only (clonal and non-clonal cells) within a single mushroom body. In wildtype, 25.5% of the total strong Mamo expressing cells (α'β' neurons) are within a clone. In *EcR-DN* clones driven by *mb-Gal4*, only 3.4% of α'β' neurons are within a clone. In *EcR-DN* clones driven by *NB + mb2-Gal4*, 24.6% of α'β' neurons are within a clone, similar to wildtype. Data in **F** are plotted as whisker plots with the same constraints as in Figure 1. A Tukey test was performed. Reported significance is compared to wildtype. ***p<0.001, ns: not significant.

neuroblasts co-stained for the pan-neuroblast marker Deadpan (Dpn) (Figures 3A-A', S4A-A'). However, EcR was present in mushroom body neurons, consistent with previous reports (Figures 3B-B', S4B-B') (Lee et al., 2000; Liu et al., 2015; Marchetti and Tavosanis, 2017). This likely explains why Imp and Syp levels were not affected by the presence of EcR-DN (Figures 2A-D, S3A-A'). To further confirm that this was not due to weak expression of *mb-Gal4* in neuroblasts, we constructed MARCM stocks containing *inscuteable-Gal4* (referred to as *NB-Gal4*) to drive strong expression of *UAS-EcR-DN* in neuroblasts. Because *NB-Gal4* is not expressed in the adult, we used *R13F02-Gal4* (referred to as *mb2-Gal4*), to label all adult mushroom body neuronal types (Jenett et al., 2012). Neurons positioned in close proximity to mushroom body neuroblasts (*i.e.* newborn) during development were not labeled by *NB-Gal4 + mb2-Gal4* but were labeled by *mb-Gal4* (compare arrows in Figures S4C-D'). More mature neurons further away from the neuroblasts were labeled by both drivers. We induced wildtype and *EcR-DN* clones at L1 with *NB-Gal4 + mb2-Gal4* and compared GFP+ axonal morphologies to wildtype axonal morphologies marked by FasII expression in the adult. We also quantified the number of α'β' neurons by strong Mamo expression. As we already described above, only 3.4% of α'β' neurons were within *EcR-DN* clones when *mb-Gal4* was used (n=6) (Figures 3C, 3F). In comparison, *EcR-DN* clones driven by *NB-Gal4 + mb2-Gal4* (n=6) contained 24.6% of all α'β' neurons, similar to the 25.5% in wildtype clones driven by *mb-Gal4* (n=7) (Figures 3D-F). The remodeling defect of γ neurons was observed in both cases, consistent with the fact that *mb-Gal4* and *NB-Gal4 + mb2-Gal4* both drive expression in γ neurons at L3 (Figures 3C, 3E, S4C-D'). Taken together, these results demonstrate that EcR is not required in neuroblasts (and is not expressed there) to specify α'β' neurons but that it rather acts only in differentiating neurons.

This result is in contrast with our observation that Babo acts in mushroom body neuroblasts during L3, leading to a strong decrease in Imp without significantly affecting Syp, causing a difference in the Imp to Syp ratio (Figures 2E-H, S3B-B'). However, previous studies have shown that Babo induces expression of EcR in remodeling γ neurons, indicating that it can act independently in neuroblasts and in neurons (Zheng et al., 2003). To test if Babo, like EcR, also functions in α'β' neurons to specify their fate, we characterized the morphology of neurons born from ganglion mother cell (GMC) clones induced during late L3, the time in which α'β' neurons are born. GMCs are intermediate progenitors that are derived from neuroblasts but divide only

once to produce two neurons. In this way, we made only one or two prospective α'β' neurons *babo* mutant without affecting mushroom body neuroblasts (see Methods). In comparison to neuroblast clones induced at L1, α'β' neurons were present in *babo* GMC clones induced at L3, observable by axonal projections into the Trio labeled α'β' lobes (Figure S4E-E'). As a positive control for the efficiency of *babo* GMC clones, we also made *babo* GMC clones at L1 to target γ neurons: Their axons remained unpruned as expected based on previous reports (Figure S4F-F') (Zheng et al., 2003). Taken together, these results show that Babo only acts in mushroom body neuroblasts, while EcR acts in differentiating mushroom body neurons, to specify α'β' fate.

Low Imp levels activate the expression of EcR to specify α'β' neurons

We have shown that both Babo and EcR are important for α'β' specification: Babo acts in mushroom body neuroblasts to lower Imp levels while EcR acts in differentiating neurons. Since both *babo* and *EcR-DN* mutants lack α'β' neurons, Babo might down-regulate Imp in neuroblasts, which could in turn allow EcR expression in neurons. To determine whether this was the case, we knocked-down by RNAi or overexpressed *Imp* or *Syp* in all mushroom body cells with *mb-Gal4* and characterized EcR expression at wandering L3 (Figures 4A-E) (Liu et al., 2015). It has already been shown that Imp and Syp are both required for α'β' specification, results that we confirmed (Figure S5) (Liu et al., 2015). Knockdown or overexpression of *Imp* resulted in the loss of EcR in all mushroom body neurons at L3, demonstrating that the maintenance of specific Imp levels, not simply its presence or absence, is important for the expression of EcR (Figures 4B-C). Surprisingly, neither *Syp* knockdown nor *Syp* overexpression affected EcR expression (Figures 4D-E). Furthermore, we assessed Mamo expression at L3 as a marker for α'β' identity (Liu et al., 2019). Similar to EcR expression, Mamo expression was missing in *Imp* knockdown or overexpression assays (Figures 4B'-C'). In contrast, *Syp* knockdown, but not its overexpression, resulted in the absence of Mamo expression (Figures 4D'-E'). Taken together, these results show that α'β' specification requires low Imp levels to activate EcR and Syp to stabilize *mamo* transcripts, the latter which has been recently reported (Liu et al., 2019).

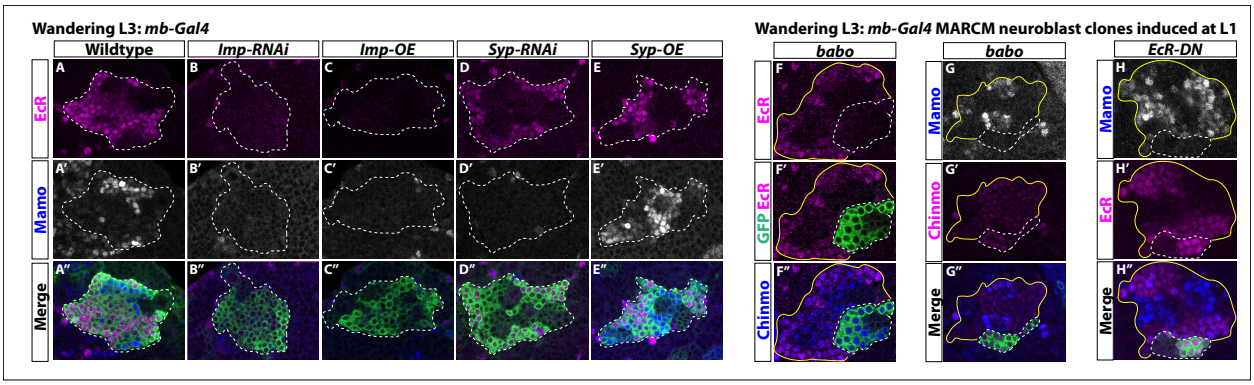

Figure 4. Imp and Syp levels regulate the expression of α'β' effectors. A-A''. Representative image of wildtype mushroom body neurons labeled by *mb-Gal4* driving *UAS-CD8::GFP* (green, white-dashed outline) during the wandering L3 stage in which EcR (magenta) and Mamo (blue, gray in single channel) are expressed. **B-B''.** When *mb-Gal4* is used to drive *UAS-Imp-RNAi*, both EcR and Mamo are not expressed. **C.** Similarly, EcR and Mamo expression are lost with *UAS-Imp-overexpression* (*OE*). **D.** *UAS-Syp-RNAi* does not affect EcR expression but does lead to the loss of Mamo. **E.** *UAS-Syp-overexpression* (*OE*) does not affect EcR or Mamo. **F.** At wandering L3, *babo* mutant clones marked by *UAS-CD8::GFP* (green, white-dashed line) driven by *mb-Gal4* do not express EcR (magenta). Mushroom body cells outside the clone and marked by Chinmo (blue, yellow line) do express EcR however **G.** Mamo (blue, gray in single channel) is not expressed at wandering L3 in *babo* clones marked by *UAS-CD8::GFP* (green, white-dashed line) driven by *mb-Gal4* but is in surrounding wildtype mushroom body neurons marked by Chinmo (magenta, yellow line). **H.** Mamo (blue, gray in single channel) is not expressed in *UAS-EcR-DN* expressing clones marked by *UAS-CD8::GFP* (green, white-dashed line) driven by *mb-Gal4* but is in wildtype mushroom body neurons marked by Chinmo (magenta, yellow line).

We have shown that Activin signaling mediated through Babo speeds up the lowering of Imp in mushroom body neuroblasts at L3, which is required to allow EcR expression in neurons fated as α'β' at this time. To further test whether Babo in neuroblasts affects EcR expression in neurons, we induced *babo* neuroblast clones at L1 and analyzed EcR at wandering L3. Consistent with previous reports and our model, we could not detect neuronal EcR expression in *babo* mutant clones (Figures 4F-4F''). In the same manner, Mamo was not expressed in *babo* mutant clones, indicating the loss of α'β' identity (Figures 4G-G''). Since Babo controls EcR expression by downregulating Imp levels, we next asked whether Mamo acts upstream or downstream of EcR to specify α'β' fate. For this, we induced *EcR-DN* clones at L1 and characterized Mamo expression at L3. Mamo was not expressed in *EcR-DN* mutant neurons compared to surrounding wildtype neurons (Figures 4H-4H''). Taken together, these results show that Activin signaling is important for allowing the expression of EcR in neurons by lowering Imp levels in neuroblasts. Ecdysone signaling via EcR then induces the expression of Mamo, which is necessary to specify α'β' identity (Liu et al., 2019).

Restoring EcR together with increasing Syp in *babo* mutants partially rescues α'β' specification

If EcR were to be the main factor required for α'β' specification, we should be able to rescue the missing α'β' neurons in *babo* neuroblast mutants by restoring *EcR* expression in neurons. We therefore induced *babo* mutant neuroblast clones and expressed *UAS-EcR*. We compared this rescue to *babo* neuroblast clones expressing *UAS-babo*. To ascertain whether our rescues were successful, we characterized GFP+ axonal morphologies of adult mushroom body neurons, focusing specifically on the α' and β' lobes (Figure 5). Additionally, we quantified the rescue phenotype by assessing the number of strong Mamo+ neurons within clones in the adult (Figure 5G). As we reported above, the percentage of α'β' neurons within wildtype neuroblast clones (n=7) was 25.5%, while in *babo* neuroblast clones (n=8) it was 2.2%. The expression of *UAS-babo* in *babo* mutant clones (n=6) nearly fully rescued the missing α'β' neuron phenotype (n=6, average: 21.1%), as well as the γ neuron remodeling phenotype (Figures 5A-5C, 5G). In contrast, the expression of *UAS-EcR* alone in *babo* mutant clones (n=8, average: 4.4%) did not significantly rescue α'β' identity but did rescue the remodeling defect of γ neurons (Figures 5D, 5G). This result shows that EcR is not sufficient to rescue the missing α'β' phenotype, implying that Babo and/or low Imp regulate the expression of additional genes required for α'β' specification. It also indicates that γ neurons are not affected in *babo* mutants other than through their inability to express EcR at L3, which is expressed much later after their specification.

Although *babo* mutants have higher Imp levels at L3, reducing Imp with RNAi led to the loss of α'β' neurons (Figures 4B, S5B)(Liu et al., 2015). Thus, removing Imp in *babo* mutant clones was not an option to rescue α'β' identity. However, since *babo* mutants have a higher Imp to Syp ratio, and this ratio is proposed to regulate α'β' identity (Liu et al., 2015), we asked whether lowering this ratio by overexpressing *Syp* in *babo* mutant clones could rescue the missing α'β' phenotype. Importantly, although Imp and Syp partially repress each other, overexpression of *Syp* with *mb-Gal4* did not lead to the loss of α'β' neurons (Figure S5E) (Liu et al., 2015). We found that *Syp* overexpression alone, like *EcR* expression alone, did not rescue the loss of α'β' neurons in *babo* clones (n=7, average: 1.8%) (Figures 5E, 5G). Unlike the *EcR* rescue, γ neurons remained unpruned. We speculate that in this rescue condition, high Imp levels at L3 prevent the expression of EcR, which is necessary to specify α'β' neurons. This result is consistent with our model that the absolute level of Imp (*i.e.*, low) is necessary for α'β' specification, not only a low Imp to Syp ratio.

Finally, we tested whether overexpressing *EcR* while increasing *Syp* in *babo* mutants would rescue α'β' neurons, reasoning that expressing *EcR* would partially restore the function of low Imp while overexpressing *Syp* would provide a lower Imp to Syp ratio. Indeed, a weak but significant rescue of the missing α'β' neuron phenotype was observed when *Syp* and *EcR* were expressed together in *babo* mutant clones (n=13, average: 6.3%) (Figure 5F-G). This small rescue highlights that the α'β' temporal window is extremely sensitive to both the Imp to Syp ratio, as

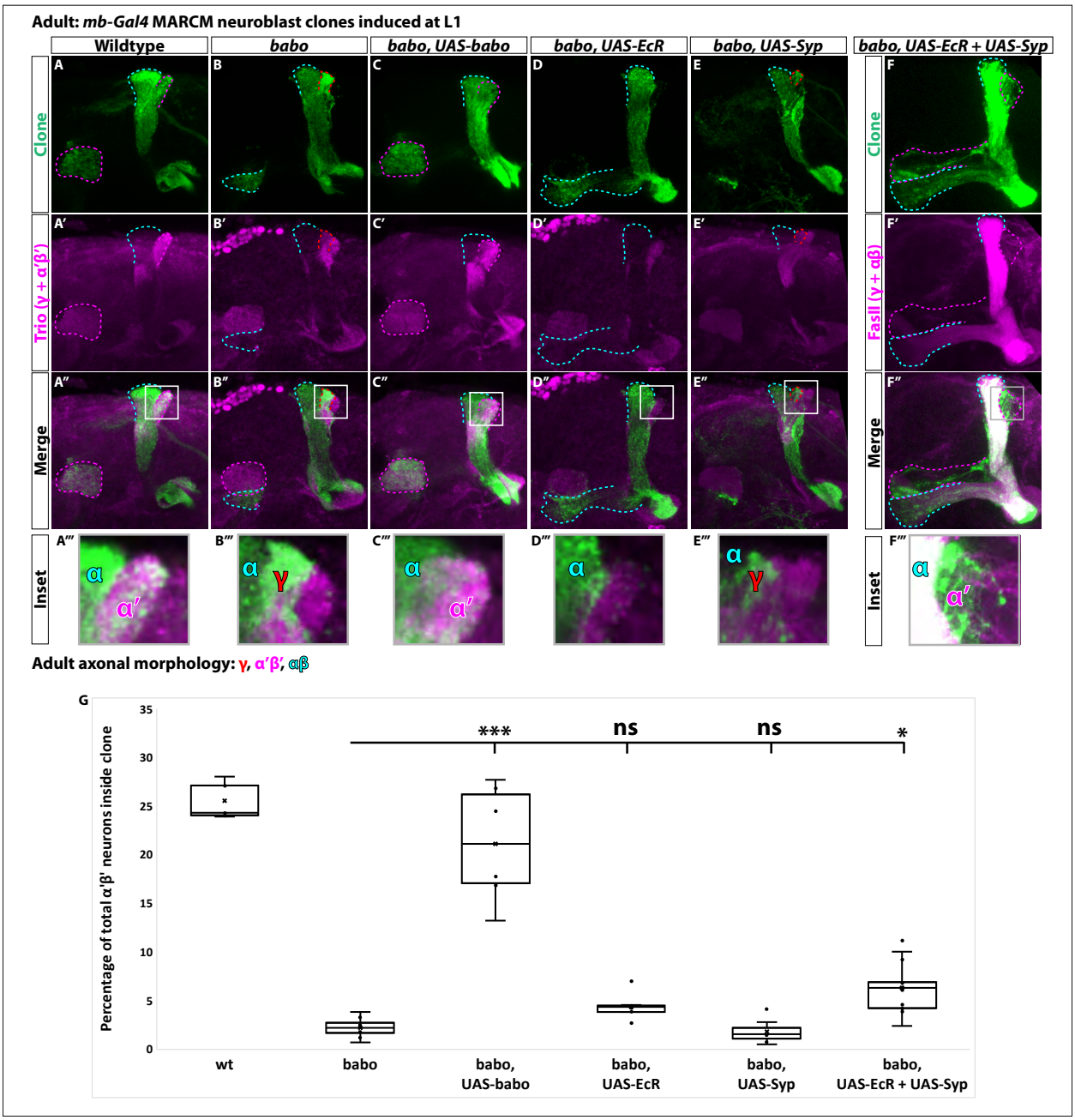

Figure 5. α'β' neurons are partially restored in *babo* mutants by co-expression of *EcR* and *Syp*. A-F. Representative maximum-projection images of adult mushroom body lobes from *mb-Gal4* MARCM clones induced at L1, focused on the α' and β' lobes. Clonally related neurons are GFP+ (green). All mushroom body axons, both clonal and non-clonal, are marked by either Trio (**A-E**) or FasII (**F**, magenta). Outlines mark GFP+ axons, where γ axons are outlined in red, α'β' axons are outlined in magenta, and αβ axons are outlined in cyan. A gray box outlines the Inset panel. **A.** In wildtype, GFP+ axons are observed in the α'β' lobes (magenta outline). **B.** In *babo* mutants, γ neurons do not remodel (red outline) and α'β' neurons are missing. **C.** These phenotypes are rescued by expressing *UAS-babo* inside mutant clones, as GFP+ axons colocalize within the Trio labeled α'β' lobes (magenta outline). **D.** α'β' neurons are not rescued by expressing *UAS-EcR*, although γ neurons remodel (seen as the absence of a vertical projection that is GFP+ and Trio+). **E.** Expression of *UAS-Syp* neither rescues the γ neuron remodeling defect nor the loss of α'β' neurons. **F.** Expression of *UAS-Syp* and *UAS-EcR* together partially rescues the loss of α'β' neurons. FasII is used to label the αβ lobes (magenta). GFP+ axons (green) localize in the αβ lobes (magenta, cyan outline). GFP+ axons from α'β' neurons (green) project adjacent to the α lobe and in front of the β lobe (magenta outline, GFP+ and FasII-). **G.** Quantification of MARCM clones represented in **A-F**. Plotted is the percentage of strong Mamo+ and GFP+ cells (clonal cells) versus all Mamo+ cells (clonal and non-clonal cells) within a single mushroom body. The number of α'β' neurons is quantified in wildtype (n=7, replotted from data in Figure 1H), *babo* (n=8, replotted from data in Figure 1H), *babo*, *UAS-babo* (n=6), *babo*, *UAS-EcR* (n=8), *babo*, *UAS-Syp* (n=7) and *babo, UAS-EcR*, *UAS-Syp* (n=13) conditions. In wildtype, 25.5% of the total strong Mamo expressing cells (α'β' neurons) are within a clone while they only represent 2.2% in *babo* clones. Expressing *UAS-babo* rescues to 21.1%. In contrast, expression of *UAS-EcR* (4.4%) or *UAS-Syp* (1.8%) alone is not statistically different from *babo*. Rescuing with *UAS-EcR* and *UAS-Syp* together however raises the percentage of α'β' neurons within the clone to 6.3%, a partial but statistically significant result. Significance values were determined using a Tukey test. Reported significance is compared to *babo*. Whisker plots follow the same constraints as in Figure 1. ***$p<0.001$, *$p<0.05$, ns: not significant.

well as to absolute Imp levels. It also indicates that multiple effector genes converge to specify α'β' fate.

In conclusion, we describe a novel mechanism used to generate neuronal diversity in *Drosophila*: the incorporation of an extrinsic signal (Activin) in neuroblasts modifies an intrinsic temporal factor (Imp) to control the expression of downstream effector genes (e.g., EcR) in neurons and thus neuronal identity (α'β') (Figure 6). Disrupting either Activin or Ecdysone pathways affects temporal identity but in different manners: *babo* loss-of-function leads to fewer αβ neurons and likely additional γ neurons, presumably because Imp levels remain high for too long (modeled in Figure 6). In contrast, *EcR-DN* clones lead to additional αβ neurons (Marchetti and Tavosanis, 2017), as EcR cannot affect the Imp to Syp ratio in mushroom body neuroblasts at L3 and leads to neurons that are better primed to adopt an αβ fate (modeled in Figure S6A-B). Our results illustrate that neuronal diversity can be generated by adding an extrinsic cue onto an intrinsic temporal sequence and show that extrinsic cues can act beyond timing temporal transitions during neurogenesis.

Discussion:

Regulating temporal identity: the role of extrinsic cues

We show here that the production of the three major mushroom body neuronal types is regulated by intrinsic and extrinsic cues during development (Figure 6). Intrinsic temporal patterning in the central brain, including in the mushroom bodies, is regulated through opposing gradients of Imp and Syp in neuroblasts (Liu et al., 2015; Ren et al., 2017; Syed et al., 2017a). Conceptually, how Imp and Syp gradients translate into different neuronal identities through time has been compared to how morphogen gradients pattern tissues in space, for instance patterning of the anterior-posterior axis of the *Drosophila* embryo, where the Bicoid morphogen positioned at the anterior pole of the egg, and Nanos at the posterior, are converted into discrete spatial domains that define cell fate (Briscoe and Small, 2015; Liu et al., 2019). In brain neuroblasts, Imp and Syp are temporal "morphogens" that can roughly separate young and old temporal states. It is unclear how the various neuronal types that are produced by the majority of neuroblasts can arise from just two

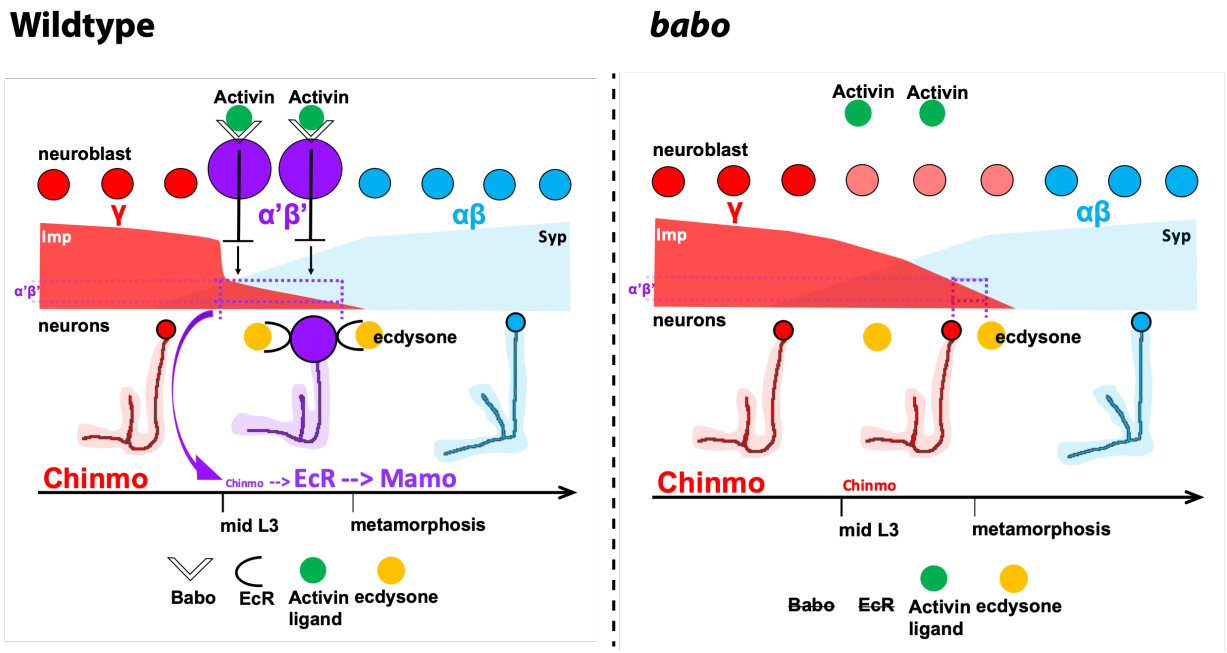

Figure 6. Model of how Activin signaling defines the mid-temporal identity window. In wildtype, as development proceeds, mushroom body neuroblasts incorporate an extrinsic cue (Activin) through Babo to lower the level of the intrinsic temporal factor Imp. The lower Imp levels inherited by newborn neurons promote EcR expression through low Chinmo levels. Ecdysone signaling through EcR then controls the expression of the α'β' effector Mamo to define the mid-temporal window (magenta dashed lines). In *babo* mutants, Imp remains higher for longer, leading to the loss of EcR and thus Mamo during late L3 in neurons. In this scenario, γ neurons are increased, α'β' neurons are lost and fewer αβ neurons are produced (magenta dashed lines). However, the Imp to Syp transition still occurs, allowing for young (γ) and old (αβ) fates to be produced.

broad temporal windows. An intriguing hypothesis is that perhaps similarly to how the gap genes in the *Drosophila* embryo act downstream of the anterior-posterior morphogens, tTF series could act downstream of the two broad temporal windows (Liu et al., 2019). However, we show in the mushroom body lineage, where only three main neuronal types are produced for dozens to hundreds of divisions from a single neuroblast, that extrinsic cues can act directly on the intrinsic program to convert two broad temporal windows into three to define an additional neuronal type. Although mushroom body neurogenesis is unique and simple, subdividing broad temporal windows by incorporating extrinsic cues may be a simple way to increase neuronal diversity in other central brain lineages.

We propose that, during the early stages of mushroom body development, high Imp levels are translated into high Chinmo levels to specify γ identity. As in other central brain neuroblasts, as development proceeds, intrinsic but weak inhibitory interactions between Imp and Syp help create a slow decrease of Imp and a corresponding increase of Syp. However, at the end of the γ window, Activin signaling through Babo acts to rapidly reduce Imp levels without affecting Syp, establishing a period of low Imp (and thus low Chinmo) and also low Syp. This is required for activating effector genes, including EcR, in prospective α'β' neurons, allowing them to respond to the peak of ecdysone at this stage that then regulates additional effectors such as Mamo, which is stabilized by Syp (Liu et al., 2019). The production of αβ identity begins when Imp (and thus Chinmo) are further decreased and Syp levels are high, as well as from ecdysone input directly in αβ neurons (Figure 6) (Kucherenko et al., 2012; Marchetti and Tavosanis, 2017; Wu et al., 2012). In the absence of Babo, low Imp levels are only reached later, thus explaining the decreased number of αβ neurons and the likely increase of γ neurons.

In non-mushroom body central brain neuroblasts, the absolute transition from Imp to Syp is controlled by a member of the intrinsic temporal series, Seven-up (Svp), and thus it functions as a switching factor (Dillard et al., 2018; Kanai et al., 2005; Maurange et al., 2008; Narbonne-Reveau et al., 2016; Ren et al., 2017; Syed et al., 2017a). The exact timing of the Imp to Syp transition in central brain neuroblasts however is controlled by extrinsic signaling through EcR, which is downstream of Svp. Thus, the function of ecdysone is to time the Imp to Syp switch, but it is not necessary for it since it still occurs in the presence of EcR-DN, although delayed (Dillard et al., 2018; Syed et al., 2017a). It is not known whether neuronal diversity is affected when ecdysone signaling is blocked in these lineages (Syed et al., 2017a). Interestingly, Svp does not

play the same role during mushroom body development, as all three neuronal types were present in *svp* mutant clones (Figure S1I). Similar to how ecdysone signaling promotes the Imp to Syp transition in most central brain neuroblasts, Activin signaling promotes the Imp to Syp transition in mushroom body neuroblasts. In both cases however, blocking reception of either only delays the transition. For example, we showed that Imp levels declined and Syp levels increased through time in mushroom body neuroblasts regardless of whether they received Activin input (Figure S3I-J). Although there is an antagonistic relationship between Imp and Syp, it does not appear to be enough to account for the absolute Imp to Syp transition. However, this interaction is likely important for creating discrete, young versus old temporal windows, which are observed by the binary expression of factors such as Chinmo and Broad in neurons (Liu et al., 2015; Maurange et al., 2008; Syed et al., 2017a). Thus, the role of the extrinsic Activin cue during mushroom body development is twofold: First, to modify the intrinsic program to create a temporal window that otherwise could not exist (*i.e.*, an extended low Imp, low Syp window), and second, to time the Imp to Syp transition (like ecdysone in other central brain neuroblasts).

Mamo expression in mushroom body neurons was recently shown to be a marker of mid-temporal fate, labeling α'β' neurons from the time of their birth (Liu et al., 2019). As the α'β' temporal window extends from mid L3 to pupation, may neurons are Mamo+. In comparison, in antennal lobe lineages that produce highly diverse projection neurons as part of the olfactory processing system, Mamo only labels a handful of neurons during development (Liu et al., 2019). This could mean that the majority of central brain neuroblasts have a very short, mid-temporal phase (Liu et al., 2015; Ren et al., 2017; Syed et al., 2017a; Yang et al., 2017). The role of Activin signaling during mushroom body development can be interpreted as extending the mid-temporal phase by promoting the decrease of Imp levels without leading to a corresponding increase in Syp levels, leading to many more neurons with mid-temporal identity (*i.e.* α'β' neurons). It will be interesting to test whether an extended mid-temporal phase could be induced by extrinsic signals in non-mushroom body neuroblasts and whether this would lead to new neuronal types. For example, since expressing EcR-DN in non-mushroom body neuroblasts leads to prolonged Imp expression and an extension of neuroblast life (Dillard et al., 2018; Homem et al., 2014; Syed et al., 2017a), perhaps these neuroblasts maintain a longer mid-temporal window that includes novel neuronal types, which could be initially monitored by Mamo expression.

Local or systemic Activin ligand(s) could act on mushroom body neuroblasts

Our finding that Activin signaling plays an important role in specifying mid-temporal identity during mushroom body development leads to the question of where the ligand originates. Our initial hypothesis that we are still exploring, is that glia are the source since they are already known to produce the Activin ligand Myoglianin necessary for the remodeling of mushroom body γ neurons (Awasaki et al., 2011). However, our initial attempts to knockdown individual Activin ligands from glia have not led to the loss of α'β' neurons, although we could recapitulate the γ neuron remodeling defect (Figure S6C-D). In the vertebrate cortex, one mechanism for switching temporal identity is through feedback from earlier born neurons in order to control the number of neurons produced (Parthasarathy et al., 2014; Seuntjens et al., 2009; Toma et al., 2014; Wang et al., 2016). However, knocking-down a combination of Activin ligands from mushroom body neurons did not result in the loss of α'β' neurons (Figure S6E). It is possible that Activin ligands act redundantly or that multiple sources exist. Thus, simultaneously knocking-down combinations of Activin ligands from multiple sources may be necessary to elicit a phenotype. It is also possible that whichever Activin ligands are used, they might not be generated from a local source and might instead be systemic, given that mushroom body temporal windows are constrained within developmental stages. Although Activin signaling is typically thought to be a short-range signaling pathway, TGFβ ligands can act systemically (Upadhyay et al., 2017). For example, it was recently shown in *Drosophila* that the BMP ligand Dpp, emanating from larval imaginal discs, acts as a developmental timer: as the animal grows, systemic Dpp is trapped by larger tissues, which is sensed by the ecdysone releasing organ to regulate entry into metamorphosis (Setiawan et al., 2018). The potential importance of local and/or systemic Activin ligands and how they might affect neuronal diversity and temporal patterning will be the topic of future investigations.

Mechanisms to define mushroom body neuronal subtypes

In this study, we have focused on the three main classes of mushroom body neurons. However, it is known that at least 7 subtypes exist: 2 γ, 2 α'β' and 3 αβ (Aso et al., 2014). These subtypes are distinguishable based on slightly different morphologies and by a few molecular markers in the adult. Interestingly, single cell sequencing of the adult central brain cannot (as of now) segregate beyond the three main classes, suggesting highly similar transcriptional profiles between neuronal subtypes (at least in the adult) (Croset et al., 2018). The mechanisms through which these neuronal

subtypes are specified is unknown. We do know that the subtypes are specified sequentially, ruling out the possibility of a stochastic process controlling subtype identity within each of the three temporal windows (Aso et al., 2014). Thus, it is likely that each of the three broad mushroom body temporal windows can be subdivided further, either by additional extrinsic cues or perhaps by a tTF series. Finding candidate tTFs will be aided by performing single neuronal cell sequencing through several development stages to increase temporal resolution.

Shared mechanisms of temporal patterning during neurogenesis between invertebrates and vertebrates

It is well established that extrinsic cues play important roles during vertebrate neurogenesis, either by regulating temporal competence of neural stem cells or by controlling the timing of temporal identity transitions (Kawaguchi, 2019). Competence changes mediated by extrinsic cues were demonstrated in classic heterochronic transplantation studies that showed that young donor progenitors produce old neuronal types when placed in older host brains. (Desai and McConnell, 2000; Frantz and McConnell, 1996; McConnell, 1988). Recent studies show that the reverse is also true when old progenitors are placed in a young environment (Oberst et al., 2019). The progressive restriction of competence in some vertebrate progenitors is similar to *Drosophila* VNC neuroblasts, which are only competent to produce early neurons for a limited number of cell divisions (Cleary and Doe, 2006; Kohwi et al., 2011, 2013; Meng et al., 2019). The role of extrinsic cues in timing temporal transition was recently demonstrated in the vertebrate hindbrain, where neural stem cells progressively produce motor neurons followed by serotonergic neurons before switching to producing glia (Chleilat et al., 2018; Dias et al., 2014). The motor neuron to serotonergic neuron switch is fine-tuned by TGFβ signaling, similar to how ecdysone and Activin fine-tune the Imp to Syp transition in *Drosophila* central brain and mushroom body neuroblasts. However, in the mushroom bodies, we showed that Activin signaling also defines a new temporal window to increase neuronal diversity. Since it is likely that many more neuronal types exist within the broad motor and serotonergic neuronal categories in vertebrates, it would be interesting to determine if neuronal subtypes are lost in TGFβ mutants, similar to how mid-temporal identity is lost in the mushroom bodies in Activin receptor mutants.

In addition to similarities in extrinsic temporal patterning, mechanisms of intrinsic temporal patterning are also conserved (Alsio et al., 2013; Elliott et al., 2008; Konstantinides et

al., 2015; Mattar et al., 2015; Shen et al., 2006). For example, vertebrate retinal progenitor cells use an intrinsic tTF cascade to bias young and old retinal fates (Elliott et al., 2008; Mattar et al., 2015). tTF series also seem to exist in cortical radial glia progenitors and even in the nerve cord (Delile et al., 2019; Gao et al., 2014; Llorca et al., 2019; Telley et al., 2016, 2019). Recent results also show the importance of post-transcriptional regulation in defining either young or old cortical fates (Shu et al., 2019; Zahr et al., 2018), which can be compared to the use of posttranscriptional regulators that are a hallmark of neuronal temporal patterning in *Drosophila* central brain neuroblasts. These studies highlight how the mechanisms driving the diversification of neuronal types are conserved while providing hope that a finite number of methods are used to build brains of all sizes and complexity and that we are closer to understanding them.

Acknowledgements:

We would like to thank the fly community, the Bloomington and the DGRC stock centers for flies and reagents; Nikos Konstantinides for discussion throughout the project and comments on the manuscript. Tzumin Lee for sharing data prior to publication; Tzumin Lee, Lynn Riddiford, Oren Schuldiner and Michael B. O'Connor for fly stocks; Tzumin Lee and Cedric Maurange for antibodies. We would like to thank all the Desplan lab members for their discussion and comments on the manuscript; Funding: This work was supported by grants from NIH (R01 EY017916 and R21 NS095288). A.M.R. was partly supported by funding from NIH (T32 HD007520), and by NYU's GSAS MacCracken Program and a Dean's Dissertation Fellowship.

Author contributions:

Conceptualization, A.M.R. and C.D.; Investigation, A.M.R.; Writing - Original Draft, A.M.R.; Writing - Review and Editing, A.M.R. and C.D.; Data and materials availability: All data are available in the main text or supplementary materials.

Declaration of Interests:

The authors declare no competing interests.

Methods:

***Drosophila* strains and MARCM**

Flies were kept on standard cornmeal medium at 25°C. For MARCM experiments, embryos were collected every 12 hours. After 24 hours, L1 larvae were placed at 37°C for 2 hours for neuroblast clones or 15 minutes for GMC clones. To target GMCs at L3, larvae were aged for 84 hours and then placed at 37°C for 15 minutes. Brains were dissected from 1-5 day old adults.

We used the following transgenic and mutant flies in combination or recombined in this study. {} enclose individual genotypes, separated by commas. Stock numbers refers to BDSC unless otherwise stated:

{*y, w, UAS-mCD8::GFP, hsFlp; FRTG13, tub-Gal80/CYO; ; OK107-Gal4* (gift from Oren Schuldiner)}, {*hsFLP, y, w; FRTG13, UAS-mCD8::GFP* (#5131)}, {*hsFLP, tubP-GAL80, w, FRT19A; UAS-mCD8::GFP/CyO; OK107-Gal4* (#44407)}, {*hsFLP, y, w, UAS-mCD8::GFP; FRT82B, tubP-GAL80/TM3, Sb*^{1}*; OK107-Gal4* (#44408)}, {*hsFLP, y*^{1}*, w*, UAS-mCD8::GFP; tubP-GAL80, FRT40A; OK107-Gal4* (#44406)}, {*UAS-EcR.B1-DeltaC655.W650A* (#6872)}, {*y, w, FRT19A* (#1744)}, {*FRTG13, babo*^{52} (gift from Dr. Michael B. O'Connor)}, {*w; FRTG13* (#1956)}, {*w1118; repo-Gal4/TM3, Sb*^{1} (#7415)}, {w; *GMR71G10-GAL4* (#39604)}, {w; *GMR41C07-GAL4/TM3, Sb*^{1} (#48145)}, {*w; GMR13F02-GAL4* (#48571)}, {*w; GMR44E04-GAL4* (#50210)}, {*w*; insc-Gal4*^{Mz1407} (#8751)}, {*usp*^{2}*/FM7a* (#31414)}, {*Met*^{27}*, gce*$^{2.5K}$*/FM7c, 2xTb*^{1}*-RFP, sn*$^{+}$ (gift from Dr. Lynn Riddiford)}, {*y*^{d2}*, w*^{1118}*, ey-FLP; tai*^{EY11718} *FRT40A/CyO, y*$^{+}$ (DGRC #114680)}, {*dpy*^{ov1}*, tai*^{61G1}*, FRT40A/CyO* (#6379)}, {*w*; smo*^{119B6}*, al*^{1}*, dpy*^{ov1}*, b*^{1}*, FRT40A/CyO* (#24772)}, {*FRT82B, svp*^{1}*/TM3* (gift from Tzumin Lee)}, {*y*^{1}*, w*, UAS-mCD8::GFP, Smox*^{MB388}*, FRT19A/FM7c* (#44384)}, {*w*;; UAS-p35* (#5073)}, *{y*^{1}*, w; Mi{PT-GFSTF.1}EcR[MI05320-GFSTF.1]/SM6a,* (#59823)}, {*y*^{1}*, w*; Pin*^{Yt}*/CyO; UAS-mCD8::GFP* (#5130)}, {*w*; ; UAS-EcR.B1* (#6469)}, {*y, w; ; UAS-babo-a/TM6* (gift from Dr. Michael O'Connor)}, {*UAS-Imp-RNAi* (#34977, gift from Dr. Tzumin Lee)}, {*UAS-Imp-RM-Flag* (gift from Dr. Tzumin Lee)}, {*UAS-Syp-RNAi* (VDRC 33012, gift from Dr. Tzumin Lee)}, {*UAS-Syp-RB-HA* (gift from Dr. Tzumin Lee)}, {*y*^{1}*, v*^{1}*; UAS-myoglianin-RNAi* (#31200)}, {*y*^{1}*, v*^{1}*; UAS-Activinβ-RNAi* (#42493)}, {*w*; OK107-Gal4 /In*^{4}*, ci*^{D} (#854)}.

Immunohistochemistry and microscopy

Fly brains were dissected in ice-cold PBS and fixed for 15-20 minutes in 4% Formaldehyde (v/w) in 1XPBS. Following a 2 hour wash in PBST (1XPBS + 0.3% Triton X-100), brains were incubated for 1-2 days in primary antibodies diluted in PBST, followed by overnight with secondary antibodies diluted in PBST. After washes, brains were mounted in Slowfade (Life Technologies) and imaged on either a Leica SP5 or SP8 confocal. Images were processed in Fiji and Adobe Illustrator (CC18).

We used the following antibodies in this study:
sheep anti-GFP (1:500, Bio-Rad #4745-1051), mouse anti-Trio (1:50, DSHB #9.4A anti-Trio), guinea pig anti-Mamo (1:200, this study, Genscript), mouse anti-FasII (1:50, DSHB #1D4 anti-Fasciclin II), rat anti-Imp (1:200, this study, Genscript), rabbit anti-Syp (1:200, this study, Genscript), guinea pig anti-Dpn (1:1000, Genscript), rabbit anti-FasII (1:50, this study, Genscript), mouse anti-EcR-B1 (1:20, DSHB #AD4.4(EcR-B1)), mouse anti-Dac2-3 (1:20, DSHB #mAbdac2-3), guinea pig anti-Chinmo (1:200, this study, Genscript), rat anti-Chinmo (1:200, gift from Dr. Cedric Maurange), rat anti-DNcad (1:20, DSHB #DN-Ex #8), donkey anti-sheep Alexa 488 (1:500, Jackson ImmunoResearch #713-545-147), donkey anti-mouse Alexa 555 (1:400, Thermo Scientific #A-31570), donkey anti-rabbit Alexa 555 (1:400, Thermo Scientific #A-31572), donkey anti-rat Alexa 647 (1:400, Jackson Immunochemicals #712-605-153), donkey anti-guinea pig Alexa 647 (1:400, Jackson Immunochemicals #706-605-148), donkey anti-rabbit 405 (1:100, Jackson Immunochemicals #711-475-152), donkey anti-rat Cy3 (1:400, Jackson Immunochemicals #712-165-153), donkey anti-mouse 405 (1:100, Jackson Immunochemicals # #711-475-150).

Polyclonal antibodies were generated by Genscript (https://www.genscript. com/). The epitopes used for each immunization are listed below.

Mamo: amino acids 467-636 of the full length protein:
MDDRLEQDVDEEDLDDDVVVVGPATAMARGIAQRLAHQNLQRLHHTHHHAQHQHSQ
HHHPHSQHHHTPHHQQHHTHSDDEDAMPVIAKSEILDDDYDDEMDLEDDDEADNSSN
DLGLNMKMGSGGAGGGGGVDLSTGSTLIPSPLITLPSSSAAAAAAAAAAMESQRSTPHH
HHHH

Imp: amino acids 76-455 (of isoform PB) of the full length protein:
ADFPLRILVQSEMVGAIIGRQGSTIRTITQQSRARVDVHRKENVGSLEKSITIYGNPENCT
NACKRILEVMQQEAISTNKGEICLKILAHNNLIGRIIGKSGNTIKRIMQDTDTKITVSSINDI
NSFNLERIITVKGLIENMSRAENQISTKLRQSYENDLQAMAPQSLMFPGLHPMAMMSTP
GNGMVFNTSMPFPSCQSFAMSKTPASVVPPVFPNDLQETTYLYIPNNAVGAIIGTRGSHI
RSIMRFSNASLKIAPLDADKPLDQQTERKVTIVGTPEGQWKAQYMIFEKMREEGFMCGT
DDVRLTVELLVASSQVGRIIGKGGQNVRELQRVTGSVIKLPEHALAPPSGGDEETPVHIIG
LFYSVQSAQRRIRAMML

Syp: amino acids 35-231(of isoform PA) of the full length protein:
MAEGNGELLDDINQKADDRGDGERTEDYPKLLEYGLDKKVAGKLDEIYKTGKLAHAE
LDERALDALKEFPVDGALNVLGQFLESNLEHVSNKSAYLCGVMKTYRQKSRASQQGV
AAPATVKGPDEDKIKKILERTGYTLDVTTGQRKYGGPPPHWEGNVPGNGCEVFCGKIPK
DMYEDELIPLFENCGIIWDLRLMM

FasII: amino acids 770-873 (of isoform PA) of the full length protein:
MHHHHHHDLLCCITVHMGVMATMCRKAKRSPSEIDDEAKLGSGQLVKEPPPSPLPLPPP
VKLGGSPMSTPLDEKEPLRTPTGSIKQNSTIEFDGRFVHSRSGEIIGKNSAV

Chinmo: amino acids 494-604 (of isoform PF) of the full length protein:
MLNVWNATKMNNKNSVNTADGKKLKCLYCDRLYGYETNLRAHIRQRHQGIRVPCPFC
ERTFTRNNTVRRHIAREHKQEIGLAAGATIAPAHLAAAAAASAAATAAAS
NHSPHHHHHH

Cell counts quantification

All confocal images were taken with a step size of three microns. Using Fiji, each image was cropped to limit the area to a region containing mushroom body cell bodies. In all cases, GFP+ cells were manually counted. To count α'β' neurons, images were split into their individual channels and the channel containing Mamo staining was automatically binarized to account for weak and strong Mamo expression using either Default or RenyiEntropy thresholding. Binarized images were processed further using the Watershed method to differentiate between contacting

cells. The number of particles (*i.e.,* strong Mamo cells) measuring between 50-infinity squared pixels were automatically counted using the Analyze Particles function and a separate channel containing bare outlines of the counts was produced and inverted. This method automatically produced the total number of strong Mamo+ cells. Individual channels were then remerged. Outlines drawn from the Analyze Particles function that overlapped with GFP+ cells were defined as α'β' neurons within a clone. In the eight cases where two mushroom body neuroblasts were labeled in a single hemisphere (wildtype:1, *babo*, *UAS-EcR*: 3, *babo*, *UAS-EcR*, *UAS-Syp*: 2, *babo*, *UAS-Syp*: 2), the total number of α'β' neurons within clones was divided by 2.

Imp and Syp fluorescence quantification

All brains used for quantifying Imp and Syp fluorescence values in *babo* or *EcR-DN* mutants were prepared together. Additionally, all images used for quantification were imaged using the same confocal settings for each channel. Fluorescence measurements were made in Fiji. Values for Imp and Syp were measured within the same hand-drawn area encompassing the entire neuroblast from a single z-slice.

Statistics

Statistical tests were performed in Excel or R. The exact tests used are reported in the figure legends.

<u>References</u>

Abdusselamoglu, M.D., Eroglu, E., Burkard, T.R., and Knoblich, J.A. (2019). The transcription factor odd-paired regulates temporal identity in transit-amplifying neural progenitors via an incoherent feed-forward loop. Elife *8*, 1–26.

Alsio, J.M., Tarchini, B., Cayouette, M., and Livesey, F.J. (2013). Ikaros promotes early-born neuronal fates in the cerebral cortex. Proc. Natl. Acad. Sci. *110*, E716–E725.

Alyagor, I., Berkun, V., Keren-Shaul, H., Marmor-Kollet, N., David, E., Mayseless, O., Issman-Zecharya, N., Amit, I., and Schuldiner, O. (2018). Combining Developmental and Perturbation-Seq Uncovers Transcriptional Modules Orchestrating Neuronal Remodeling. Dev. Cell *47*, 38-52.e6.

Aso, Y., Hattori, D., Yu, Y., Johnston, R.M., Iyer, N.A., Ngo, T.-T.B., Dionne, H., Abbott, L.F.,

Axel, R., Tanimoto, H., et al. (2014). The neuronal architecture of the mushroom body provides a logic for associative learning. Elife *3*, e04577.

Averbukh, I., Lai, S.-L., Doe, C.Q., and Barkai, N. (2018). A repressor-decay timer for robust temporal patterning in embryonic Drosophila neuroblast lineages. Elife *7*, 354969.

Awasaki, T., Saito, M., Sone, M., Suzuki, E., Sakai, R., Ito, K., and Hama, C. (2000). The Drosophila trio plays an essential role in patterning of axons by regulating their directional extension. Neuron *26*, 119–131.

Awasaki, T., Huang, Y., O'Connor, M.B., and Lee, T. (2011). Glia instruct developmental neuronal remodeling through TGF-β signaling. Nat. Neurosci. *14*, 821–823.

Baumann, A.A., Texada, M.J., Chen, H.M., Etheredge, J.N., Miller, D.L., Picard, S., Warner, R., Truman, J.W., and Riddiford, L.M. (2017). Genetic tools to study juvenile hormone action in Drosophila. Sci. Rep. *7*, 2132.

Bayraktar, O.A., and Doe, C.Q. (2013). Combinatorial temporal patterning in progenitors expands neural diversity. Nature *498*, 449–455.

Bello, B.C., Izergina, N., Caussinus, E., and Reichert, H. (2008). Amplification of neural stem cell proliferation by intermediate progenitor cells in Drosophila brain development. Neural Dev. *3*, 5.

Bertet, C., Li, X., Erclik, T., Cavey, M., Wells, B., and Desplan, C. (2014). Temporal Patterning of Neuroblasts Controls Notch-Mediated Cell Survival through Regulation of Hid or Reaper. Cell *158*, 1173–1186.

Boone, J.Q., and Doe, C.Q. (2008). Identification of Drosophila type II neuroblast lineages containing transit amplifying ganglion mother cells. Dev. Neurobiol. *68*, 1185–1195.

Bowman, S.K., Rolland, V., Betschinger, J., Kinsey, K.A., Emery, G., and Knoblich, J.A. (2008). The Tumor Suppressors Brat and Numb Regulate Transit-Amplifying Neuroblast Lineages in Drosophila. Dev. Cell *14*, 535–546.

Briscoe, J., and Small, S. (2015). Morphogen rules: Design principles of gradient-mediated embryo patterning. Dev. *142*, 3996–4009.

Brody, T., and Odenwald, W.F. (2000). Programmed Transformations in Neuroblast Gene Expression during Drosophila CNS Lineage Development. Dev. Biol. *226*, 34–44.

Brummel, T., Abdollah, S., Haerry, T.E., Shimell, M.J., Merriam, J., Raftery, L., Wrana, J.L., and O'Connor, M.B. (1999). The Drosophila activin receptor Baboon signals through dSmad2 and controls cell proliferation but not patterning during larval development. Genes Dev. *13*, 98–111.

Chai, P.C., Liu, Z., Chia, W., and Cai, Y. (2013). Hedgehog Signaling Acts with the Temporal Cascade to Promote Neuroblast Cell Cycle Exit. PLoS Biol. *11*.

Chleilat, E., Skatulla, L., Rahhal, B., Hussein, M.T., Feuerstein, M., Krieglstein, K., and Roussa, E. (2018). TGF-β Signaling Regulates Development of Midbrain Dopaminergic and Hindbrain Serotonergic Neuron Subgroups. Neuroscience *381*, 124–137.

Cleary, M.D., and Doe, C.Q. (2006). Regulation of neuroblast competence: multiple temporal identity factors specify distinct neuronal fates within a single early competence window. Genes Dev. *20*, 429–434.

Cognigni, P., Felsenberg, J., and Waddell, S. (2018). Do the right thing: neural network mechanisms of memory formation, expression and update in Drosophila. Curr. Opin. Neurobiol. *49*, 51–58.

Connolly, J.B., Roberts, I.J.H., Armstrong, J.D., Kaiser, K., Forte, M., Tully, T., and O'Kane, C.J. (1996). Associative learning disrupted by impaired Gs signaling in Drosophila mushroom bodies. Science (80-.). *274*, 2104–2107.

Crittenden, J.R., Skoulakis, E.M.C., Han, K.-A., Kalderon, D., and Davis, R.L. (1998). Tripartite Mushroom Body Architecture Revealed by Antigenic Markers. Learn. Mem. *5*, 38–51.

Croset, V., Treiber, C.D., and Waddell, S. (2018). Cellular diversity in the Drosophila midbrain revealed by single-cell transcriptomics. Elife *7*, e34550.

Delile, J., Rayon, T., Melchionda, M., Edwards, A., Briscoe, J., and Sagner, A. (2019). Single cell transcriptomics reveals spatial and temporal dynamics of gene expression in the developing mouse spinal cord. Development *146*.

Desai, A.R., and McConnell, S.K. (2000). Progressive restriction in fate potential by neural progenitors during cerebral cortical development. Development *127*, 2863–2872.

Dias, J.M., Alekseenko, Z., Applequist, J.M., and Ericson, J. (2014). Tgfβ Signaling Regulates Temporal Neurogenesis and Potency of Neural Stem Cells in the CNS. Neuron *84*, 927–939.

Dillard, C., Narbonne-Reveau, K., Foppolo, S., Lanet, E., and Maurange, C. (2018). Two distinct mechanisms silence chinmo in Drosophila neuroblasts and neuroepithelial cells to limit their self-renewal. Development *145*, dev154534.

Doe, C.Q. (2017). Temporal Patterning in the Drosophila CNS. Annu. Rev. Cell Dev. Biol. *33*, 219–240.

Elliott, J., Jolicoeur, C., Ramamurthy, V., and Cayouette, M. (2008). Ikaros Confers Early

Temporal Competence to Mouse Retinal Progenitor Cells. Neuron *60*, 26–39.

Eroglu, E., Burkard, T.R., Jiang, Y., Saini, N., Homem, C.C.F., Reichert, H., and Knoblich, J.A. (2014). SWI/SNF Complex Prevents Lineage Reversion and Induces Temporal Patterning in Neural Stem Cells. Cell *156*, 1259–1273.

Frantz, G.D., and McConnell, S.K. (1996). Restriction of late cerebral cortical progenitors to an upper-layer fate. Neuron *17*, 55–61.

Gao, P., Postiglione, M.P., Krieger, T.G., Hernandez, L., Wang, C., Han, Z., Streicher, C., Papusheva, E., Insolera, R., Chugh, K., et al. (2014). Deterministic Progenitor Behavior and Unitary Production of Neurons in the Neocortex. Cell *159*, 775–788.

Genovese, S., Clément, R., Gaultier, C., Besse, F., Narbonne-Reveau, K., Daian, F., Foppolo, S., Luis, N.M., and Maurange, C. (2019). Coopted temporal patterning governs cellular hierarchy, heterogeneity and metabolism in Drosophila neuroblast tumors. Elife *8*, 1–36.

Ghbeish, N., Tsai, C.C., Schubiger, M., Zhou, J.Y., Evans, R.M., and McKeown, M. (2001). The dual role of ultraspiracle, the Drosophila retinoid X receptor, in the ecdysone response. Proc. Natl. Acad. Sci. U. S. A. *98*, 3867–3872.

Grosskortenhaus, R., Pearson, B.J., Marusich, A., and Doe, C.Q. (2005). Regulation of Temporal Identity Transitions in Drosophila Neuroblasts. Dev. Cell *8*, 193–202.

Grosskortenhaus, R., Robinson, K.J., and Doe, C.Q. (2006). Pdm and Castor specify late-born motor neuron identity in the NB7-1 lineage. Genes Dev. *20*, 2618–2627.

Holguera, I., and Desplan, C. (2018). Neuronal specification in space and time. Science (80-.). *362*, 176–180.

Homem, C.C.F., Steinmann, V., Burkard, T.R., Jais, A., Esterbauer, H., and Knoblich, J.A. (2014). Ecdysone and Mediator Change Energy Metabolism to Terminate Proliferation in Drosophila Neural Stem Cells. Cell *158*, 874–888.

Isshiki, T., Pearson, B., Holbrook, S., and Doe, C.Q. (2001). Drosophila neuroblasts sequentially express transcription factors which specify the temporal identity of their neuronal progeny. Cell *106*, 511–521.

Issman-Zecharya, N., and Schuldiner, O. (2014). The PI3K class III complex promotes axon pruning by downregulating a ptc-derived signal via endosome-lysosomal degradation. Dev. Cell *31*, 461–473.

Ito, K., Awano, W., Suzuki, K., Hiromi, Y., and Yamamoto, D. (1997). The Drosophila mushroom

body is a quadruple structure of clonal units each of which contains a virtually identical set of neurones and glial cells. Development *124*, 761–771.

Jenett, A., Rubin, G.M., Ngo, T.T., Shepherd, D., Murphy, C., Dionne, H., Pfeiffer, B.D., Cavallaro, A., Hall, D., Jeter, J., et al. (2012). A GAL4-driver line resource for Drosophila neurobiology. Cell Rep *2*, 991–1001.

Kambadur, R., Koizumi, K., Stivers, C., Nagle, J., Poole, S.J., and Odenwald, W.F. (1998). Regulation of POU genes by castor and hunchback establishes layered compartments in the Drosophila CNS. Genes Dev. *12*, 246–260.

Kanai, M.I., Okabe, M., and Hiromi, Y. (2005). Seven-up controls switching of transcription factors that specify temporal identities of drosophila neuroblasts. Dev. Cell *8*, 203–213.

Kao, C.-F., Yu, H.-H., He, Y., Kao, J.-C., and Lee, T. (2012). Hierarchical Deployment of Factors Regulating Temporal Fate in a Diverse Neuronal Lineage of the Drosophila Central Brain. Neuron *73*, 677–684.

Kawaguchi, A. (2019). Temporal patterning of neocortical progenitor cells: How do they know the right time? Neurosci. Res. *138*, 3–11.

Kohwi, M., and Doe, C.Q. (2013). Temporal fate specification and neural progenitor competence during development. Nat. Rev. Neurosci. *14*, 823–838.

Kohwi, M., Hiebert, L.S., and Doe, C.Q. (2011). The pipsqueak-domain proteins Distal antenna and Distal antenna-related restrict Hunchback neuroblast expression and early-born neuronal identity. Development *138*, 1727–1735.

Kohwi, M., Lupton, J.R., Lai, S.-L., Miller, M.R., and Doe, C.Q. (2013). Developmentally Regulated Subnuclear Genome Reorganization Restricts Neural Progenitor Competence in Drosophila. Cell *152*, 97–108.

Konstantinides, N., Rossi, A.M., and Desplan, C. (2015). Common Temporal Identity Factors Regulate Neuronal Diversity in Fly Ventral Nerve Cord and Mouse Retina. Neuron *85*, 447–449.

Kraft, K.F., Massey, E.M., Kolb, D., Walldorf, U., and Urbach, R. (2016). Retinal homeobox promotes cell growth, proliferation and survival of mushroom body neuroblasts in the Drosophila brain. Mech. Dev. *142*, 50–61.

Kucherenko, M.M., Barth, J., Fiala, A., and Shcherbata, H.R. (2012). Steroid-induced microRNA let-7 acts as a spatio-temporal code for neuronal cell fate in the developing Drosophila brain. EMBO J. *31*, 4511–4523.

Kurusu, M., Maruyama, Y., Adachi, Y., Okabe, M., Suzuki, E., and Furukubo-Tokunaga, K. (2009). A conserved nuclear receptor, Tailless, is required for efficient proliferation and prolonged maintenance of mushroom body progenitors in the Drosophila brain. Dev. Biol. *326*, 224–236.

Lee, T., and Luo, L. (1999). Mosaic analysis with a repressible neurotechnique cell marker for studies of gene function in neuronal morphogenesis. Neuron *22*, 451–461.

Lee, T., Lee, A., and Luo, L. (1999). Development of the Drosophila mushroom bodies: sequential generation of three distinct types of neurons from a neuroblast. Development *126*, 4065–4076.

Lee, T., Marticke, S., Sung, C., Robinow, S., and Luo, L. (2000). Cell-autonomous requirement of the USP/EcR-B ecdysone receptor for mushroom body neuronal remodeling in Drosophila. Neuron *28*, 807–818.

Li, X., Erclik, T., Bertet, C., Chen, Z., Voutev, R., Venkatesh, S., Morante, J., Celik, A., and Desplan, C. (2013). Temporal patterning of Drosophila medulla neuroblasts controls neural fates. Nature *498*, 456–462.

Lin, S., Marin, E.C., Yang, C.-P.P., Kao, C.-F.F., Apenteng, B.A., Huang, Y., O'Connor, M.B., Truman, J.W., Lee, T., O'Connor, M.B., et al. (2013). Extremes of Lineage Plasticity in the Drosophila Brain. Curr. Biol. *23*, 1908–1913.

Liu, L., Long, X., Yang, C., Miyares, R.L., Sugino, K., Singer, R.H., and Lee, T. (2019). Mamo decodes hierarchical temporal gradients into terminal neuronal fate. Elife *8*, 1–28.

Liu, Z., Yang, C.-P., Sugino, K., Fu, C.-C., Liu, L.-Y., Yao, X., Lee, L.P., and Lee, T. (2015). Opposing intrinsic temporal gradients guide neural stem cell production of varied neuronal fates. Science (80-.). *350*, 317–320.

Llorca, A., Ciceri, G., Beattie, R., Wong, F.K., Diana, G., Serafeimidou-Pouliou, E., Fernández-Otero, M., Streicher, C., Arnold, S.J., Meyer, M., et al. (2019). A stochastic framework of neurogenesis underlies the assembly of neocortical cytoarchitecture. Elife *8*.

Marchetti, G., and Tavosanis, G. (2017). Steroid Hormone Ecdysone Signaling Specifies Mushroom Body Neuron Sequential Fate via Chinmo. Curr. Biol. *27*, 3017-3024.e4.

Mattar, P., Ericson, J., Blackshaw, S., and Cayouette, M. (2015). A Conserved Regulatory Logic Controls Temporal Identity in Mouse Neural Progenitors. Neuron *85*, 497–504.

Maurange, C., Cheng, L., and Gould, A.P. (2008). Temporal Transcription Factors and Their Targets Schedule the End of Neural Proliferation in Drosophila. Cell *133*, 891–902.

McConnell, S.K. (1988). Fates of visual cortical neurons in the ferret after isochronic and

heterochronic transplantation. J. Neurosci. *8*, 945–974.

Meng, J.L., Marshall, Z.D., Lobb-Rabe, M., and Heckscher, E.S. (2019). How prolonged expression of Hunchback, a temporal transcription factor, re-wires locomotor circuits. Elife *8*, 1–30.

Miyares, R.L., and Lee, T. (2019). Temporal control of Drosophila central nervous system development. Curr. Opin. Neurobiol. *56*, 24–32.

Narbonne-Reveau, K., Lanet, E., Dillard, C., Foppolo, S., Chen, C., Parrinello, H., Rialle, S., Sokol, N.S., and Maurange, C. (2016). Neural stem cell-encoded temporal patterning delineates an early window of malignant susceptibility in Drosophila. Elife *5*, 1–29.

Oberst, P., Fièvre, S., Baumann, N., Concetti, C., Bartolini, G., and Jabaudon, D. (2019). Temporal plasticity of apical progenitors in the developing mouse neocortex. Nature *573*, 370–374.

Pahl, M.C., Doyle, S.E., and Siegrist, S.E. (2019). E93 Integrates Neuroblast Intrinsic State with Developmental Time to Terminate MB Neurogenesis via Autophagy. Curr. Biol. 1–13.

Parthasarathy, S., Srivatsa, S., Nityanandam, A., and Tarabykin, V. (2014). Ntf3 acts downstream of Sip1 in cortical postmitotic neurons to control progenitor cell fate through feedback signaling. Development *141*, 3324–3330.

Pearson, B.J., and Doe, C.Q. (2003). Regulation of neuroblast competence in Drosophila. Nature *425*, 624–628.

Ren, Q., Yang, C.-P., Liu, Z., Sugino, K., Mok, K., He, Y., Ito, M., Nern, A., Otsuna, H., and Lee, T. (2017). Stem Cell-Intrinsic, Seven-up-Triggered Temporal Factor Gradients Diversify Intermediate Neural Progenitors. Curr. Biol. 1–11.

Rossi, A.M., Fernandes, V.M., and Desplan, C. (2017). Timing temporal transitions during brain development. Curr. Opin. Neurobiol. *42*, 84–92.

Schubiger, M., and Truman, J.W. (2000). The RXR ortholog USP suppresses early metamorphic processes in Drosophila in the absence of ecdysteroids. Development *127*, 1151–1159.

Setiawan, L., Pan, X., Woods, A.L., O'Connor, M.B., and Hariharan, I.K. (2018). The BMP2/4 ortholog dpp can function as an inter-organ signal that regulates developmental timing. Life Sci. Alliance *1*, 1–17.

Seuntjens, E., Nityanandam, A., Miquelajauregui, A., Debruyn, J., Stryjewska, A., Goebbels, S., Nave, K.A., Huylebroeck, D., and Tarabykin, V. (2009). Sip1 regulates sequential fate decisions by feedback signaling from postmitotic neurons to progenitors. Nat. Neurosci. *12*, 1373–1380.

Shen, Q., Wang, Y., Dimos, J.T., Fasano, C.A., Phoenix, T.N., Lemischka, I.R., Ivanova, N.B., Stifani, S., Morrisey, E.E., and Temple, S. (2006). The timing of cortical neurogenesis is encoded within lineages of individual progenitor cells. Nat. Neurosci. *9*, 743–751.

Shu, P., Wu, C., Ruan, X., Liu, W., Hou, L., Fu, H., Wang, M., Liu, C., Zeng, Y., Chen, P., et al. (2019). Opposing Gradients of MicroRNA Expression Temporally Pattern Layer Formation in the Developing Neocortex. Dev. Cell *49*, 764-785.e4.

Siegrist, S.E., Haque, N.S., Chen, C.-H., Hay, B. a., and Hariharan, I.K. (2010). Inactivation of Both foxo and reaper Promotes Long-Term Adult Neurogenesis in Drosophila. Curr. Biol. *20*, 643–648.

Sipe, C.W., and Siegrist, S.E. (2017). Eyeless uncouples mushroom body neuroblast proliferation from dietary amino acids in *Drosophila*. Elife *6*, 1–10.

Suzuki, T., Kaido, M., Takayama, R., and Sato, M. (2013). A temporal mechanism that produces neuronal diversity in the Drosophila visual center. Dev. Biol. *380*, 12–24.

Syed, M.H., Mark, B., and Doe, C.Q. (2017a). Steroid hormone induction of temporal gene expression in Drosophila brain neuroblasts generates neuronal and glial diversity. Elife *6*, 1–23.

Syed, M.H., Mark, B., and Doe, C.Q. (2017b). Playing Well with Others : Extrinsic Cues Regulate Neural Progenitor Temporal Identity to Generate Neuronal Diversity. Trends Genet. *xx*, 1–10.

Telley, L., Govindan, S., Prados, J., Stevant, I., Nef, S., Dermitzakis, E., Dayer, A., and Jabaudon, D. (2016). Sequential transcriptional waves direct the differentiation of newborn neurons in the mouse neocortex. Science (80-.). *351*, 1443–1446.

Telley, L., Agirman, G., Prados, J., Amberg, N., Fièvre, S., Oberst, P., Bartolini, G., Vitali, I., Cadilhac, C., Hippenmeyer, S., et al. (2019). Temporal patterning of apical progenitors and their daughter neurons in the developing neocortex. Science (80-.). *364*, eaav2522.

Toma, K., Kumamoto, T., Hanashima, C., Toma, K., and Hanashima, C. (2014). The timing of upper-layer neurogenesis is conferred by sequential derepression and negative feedback from deep-layer neurons. J. Neurosci. *34*, 13259–13276.

Tran, K.D., and Doe, C.Q. (2008). Pdm and Castor close successive temporal identity windows in the NB3-1 lineage. Development *135*, 3491–3499.

Upadhyay, A., Moss-Taylor, L., Kim, M.-J., Ghosh, A.C., and O'Connor, M.B. (2017). TGF-β Family Signaling in Drosophila. Cold Spring Harb. Perspect. Biol. *9*, a022152.

Wang, W., Jossin, Y., Chai, G., Lien, W.H., Tissir, F., and Goffinet, A.M. (2016). Feedback

regulation of apical progenitor fate by immature neurons through Wnt7-Celsr3-Fzd3 signalling. Nat. Commun. *7*, 1–11.

Wang, Y.-C., Yang, J.S., Johnston, R., Ren, Q., Lee, Y.-J., Luan, H., Brody, T., Odenwald, W.F., and Lee, T. (2014). Drosophila intermediate neural progenitors produce lineage-dependent related series of diverse neurons. Development *141*, 253–258.

Wu, Y.-C., Chen, C.-H., Mercer, A., and Sokol, N.S. (2012). let-7-Complex MicroRNAs Regulate the Temporal Identity of Drosophila Mushroom Body Neurons via chinmo. Dev. Cell *23*, 202–209.

Yamanaka, N., Rewitz, K.F., and O'Connor, M.B. (2013). Ecdysone Control of Developmental Transitions: Lessons from Drosophila Research. Annu. Rev. Entomol. *58*, 497–516.

Yang, C.-P.P., Samuels, T.J., Huang, Y., Yang, L., Ish-Horowicz, D., Davis, I., and Lee, T. (2017). Imp and Syp RNA-binding proteins govern decommissioning of Drosophila neural stem cells. Development *144*, 3454–3464.

Yu, H.-H., Kao, C.-F., He, Y., Ding, P., Kao, J.-C., and Lee, T. (2010). A Complete Developmental Sequence of a Drosophila Neuronal Lineage as Revealed by Twin-Spot MARCM. PLoS Biol. *8*, e1000461.

Yu, H.H., Awasaki, T., Schroeder, M.D., Long, F., Yang, J.S., He, Y., Ding, P., Kao, J.C., Wu, G.Y.Y., Peng, H., et al. (2013). Clonal development and organization of the adult Drosophila central brain. Curr. Biol. *23*, 633–643.

Zahr, S.K., Yang, G., Kazan, H., Borrett, M.J., Yuzwa, S.A., Voronova, A., Kaplan, D.R., and Miller, F.D. (2018). A Translational Repression Complex in Developing Mammalian Neural Stem Cells that Regulates Neuronal Specification. Neuron *97*, 520-537.e6.

Zheng, X., Wang, J., Haerry, T.E., Wu, A.Y.-H., Martin, J., O'Connor, M.B., Lee, C.-H.J., and Lee, T. (2003). TGF-beta signaling activates steroid hormone receptor expression during neuronal remodeling in the Drosophila brain. Cell *112*, 303–315.

Zhu, S., Lin, S., Kao, C.-F., Awasaki, T., Chiang, A.-S., and Lee, T. (2006). Gradients of the Drosophila Chinmo BTB-Zinc Finger Protein Govern Neuronal Temporal Identity. Cell *127*, 409–422.